

Ergodic properties of Brownian motion under stochastic resettingE. Barkai ¹, R. Flaquer-Galmés ² and V. Méndez ²¹*Department of Physics, Institute of Nanotechnology and Advanced Materials, Bar Ilan University, Ramat-Gan 52900, Israel*²*Grup de Física Estadística, Departament de Física, Facultat de Ciències, Universitat Autònoma de Barcelona, 08193 Barcelona, Spain*

(Received 28 June 2023; accepted 26 September 2023; published 1 December 2023)

We study the ergodic properties of one-dimensional Brownian motion with resetting. Using generic classes of statistics of times between resets, we find respectively for thin- or fat-tailed distributions the normalized or non-normalized invariant density of this process. The former case corresponds to known results in the resetting literature and the latter to infinite ergodic theory. Two types of ergodic transitions are found in this system. The first is when the mean waiting time between resets diverges, when standard ergodic theory switches to infinite ergodic theory. The second is when the mean of the square root of time between resets diverges and the properties of the invariant density are drastically modified. We then find a fractional integral equation describing the density of particles. This finite time tool is particularly useful close to the ergodic transition where convergence to asymptotic limits is logarithmically slow. Our study implies rich ergodic behaviors for this nonequilibrium process which should hold far beyond the case of Brownian motion analyzed here.

DOI: [10.1103/PhysRevE.108.064102](https://doi.org/10.1103/PhysRevE.108.064102)**I. INTRODUCTION**

Stochastic processes under sporadic resetting gained considerable attention [1,2]. Under certain conditions, a nonequilibrium stationary state (NESS) is found while the system still has nonzero currents [3–6]. NESS was studied extensively for many processes with resetting [1,2], for example, for Brownian motion (BM) [3,7] and run-and-tumble processes [8]. In this work, we investigate the ergodic properties of such a process [9–11]. In the first stage of our work, we discuss a connection between the theory of NESS and the statistics of renewals; in particular, we study a useful relation between the resetting problem and the so-called backward recurrence time [12]. This not only gives a simple point of view on the emerging NESSs but can be used to relate this timely problem to Dynkin's backward time limit theorem [13] and its extension [14].

We study BM, with times between resetting being independent identically distributed (IID) random variables (RVs) [4,6,15,16]. When the process is thin- or fat-tailed respectively, we find the normalized or non-normalized invariant density of this system. Using Laplace transforms, Pal, Kundu, and Evans [4] and independently Eule and Metzger [6] found the normalized NESS of this process. Our work sheds light on these normalized states by connecting them to mathematical limit theorems from the field of renewal theory, but our main contribution is with respect to the less understood non-normalized phase.

Non-normalized states were previously studied in the context of infinite ergodic theory, in both the math [17] and the physics literature [18–23]. Here our goal is to show how this tool is used in the context of the resetting paradigm. More specifically we find alternative ergodic transitions in this system. The first is anticipated, and it is found when the mean time between resetting diverges. The second takes place when the mean of the square root of time between resetting diverges. In this case the properties of the infinite measure are

modified, as also are the relations between time and ensemble averages. As explained below, this second transition is related to a competition between two mechanisms of return to the origin, namely, will the resetting control the return process, or will it be the diffusion process itself? So our goal is to explain the rich phase diagram of the ergodic properties in this system. We focus on the best-studied case, the underlying motion being BM, but while limiting ourselves to an example, the tools presented are general.

This paper is organized as follows. In the next two sections, we present the model and recap statistical properties of the backward time. NESS is discussed in Sec. IV followed by the calculation of the moments of the process in Sec. V. Section VI contains the uniform approximation and the fractional integral equation relating the density to the Green function of BM. We then briefly discuss a special case, the sharp resetting in Sec. VII. Section VIII presents the time-integrated observables, while Sec. IX gives the detailed calculation of occupation time statistics. We end with discussion and summary.

II. MODEL AND FORMAL SOLUTION

We start with a simple relation between the density of the reset-free process and the density of the process with resetting. For that aim, we will use three probability density functions (PDFs). Let $f(B, t)$ be the PDF of the backward recurrence time B at time t , $\rho(x, t)$ the PDF of the position x of the particle at time t , and $G(x, t)$ the Green function of the walker in the absence of reset. We now explain the basic properties of these functions and their significance.

A tagged particle performs one-dimensional BM between resetting events, hence

$$G(x, t) = \frac{\exp(-x^2/4Dt)}{\sqrt{4\pi Dt}} \quad (1)$$

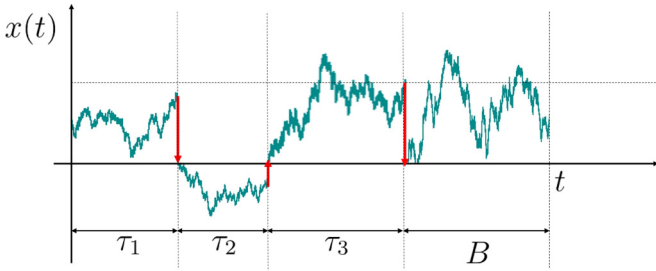


FIG. 1. Schematics of BM with resetting. Since BM is Markovian the backward recurrence time B controls the position of the restarted walker at time t . For short times, statistical properties of B will obviously depend on t ; the only exception is when the waiting times are exponentially distributed. If the time t is long, a steady state of the random variable B is found provided that the mean time between resets is finite. This in turn will determine the steady-state statistical properties of the stochastic process $x(t)$. When the mean time between resetting events diverges we are in the domain of infinite ergodic theory.

and D is the diffusion constant. This is the propagator of a free BM without resetting, the particle starting on the origin $x = 0$, at $t = 0$. The resetting is to the position $x = 0$, which is also the origin of the process. The waiting times between resetting events are independent identically distributed (IID) random variables (RVs) drawn from a common PDF of the waiting times $\psi(\tau)$. Thus at time $t = 0$ the particle starts on the origin $x(t)|_{t=0} = 0$, we draw a positive resetting time from $\psi(\tau)$ denoted τ_1 , and the particle performs a free BM in the interval of time $(0, \tau_1)$, finally reaching some random position $x(\tau_1^-)$ (the superscript $-$ indicates a time just prior to the reset). Then the particle's position is reset to zero $x(\tau_1^+) = 0$, and the process is then renewed, namely, we draw a second waiting time τ_2 also from $\psi(\tau)$, etc. When this process is continued we get the sequence of IID RVs, $\{\tau_1, \tau_2, \tau_3, \dots\}$, i.e., the waiting times between resetting events, which are needed to construct the path of the particle.

We are interested in the PDF of the position of the particle at time t denoted $\rho(x, t)$. Let $x(t)$ be the stochastic process describing the location of the particle. Since BM is a Markovian process, $x(t)$ is connected to the time the last reset to $x = 0$ was made. This last reset event is at time $t - B$ and B is called the backward recurrence time (see schematics in Fig. 1). Clearly, B is a RV, whose statistical properties in general depend on t while $0 \leq B \leq t$. In the process just described $x(t) = x^f(B)$ where $x^f(B)$ is the position of a reset free BM at time B , with the initial position $x = 0$. Hence from the well-known properties of BM, $x(t)$ for the resetting process is a product of two independent random variables \sqrt{B} and ξ ,

$$x(t) = (DB)^{1/2}\xi, \quad (2)$$

where ξ is a Gaussian RV with zero mean and variance $\langle \xi^2 \rangle = 2$. This allows for efficient sampling of the density of an ensemble of the noninteracting particles. In simulations below, we generate the backward time using the renewal process to determine statistically the location of a particle at the measurement time t , and repeating this many times we can find the sample density.

The backward time is defined according to

$$\sum_{i=1}^N \tau_i + B = t, \quad (3)$$

where N is the random number of resets in the time interval $(0, t)$; see again schematics in Fig. 1. Then using the Fourier $x \rightarrow k$ transform of $\rho(x, t)$ and Eq. (2), $\mathcal{F}[\rho(x, t)] = \langle \langle \exp(ik\sqrt{DB}\xi) \rangle \rangle_B = \langle \exp(-k^2DB) \rangle_B$ where we used the fact that B and ξ are independent RVs, and that the PDF of ξ is Gaussian. We then have

$$\mathcal{F}[\rho(x, t)] = \int_0^t f(B, t) \exp(-k^2DB) dB, \quad (4)$$

and as mentioned $f(B, t)$ is the PDF of B . Hence inverting back to x space, the formal solution to the problem reads

$$\rho(x, t) = \int_0^t f(B, t) G(x, B) dB. \quad (5)$$

Luckily statistics of B are well studied in the context of renewal theory; in particular, the PDF $f(B, t)$ is studied in [12]. Specifically, the Laplace transform of $f(B, t)$ is given in terms of the Laplace transform of $\psi(\tau)$ in [12], and some further details will be provided below.

To study nonequilibrium steady states we soon focus on the long-time limit of Eq. (5). Before doing so we note that the approach is not limited to BM in dimension one; in essence, many other transformations of B might be considered: for example, consider BM in a force field [24,25] with resetting, models of biochemical proof reading [26,27] or anomalous diffusion [28–33], a gas of particles [34], deterministic processes, etc. As explained below the waiting time strategy just described is identical to a much studied time-varying rate approach [4,6]. In all these problems the backward recurrence time plays a crucial role; hence we will soon recap some of its properties.

In this paper we will focus on two classes of resetting processes. The first are processes with a smooth PDF $\psi(\tau)$ of the reset times, when the positive integer moments of the waiting times are finite. The most studied example is $\psi(\tau) = \exp(-\tau)$ for $\tau > 0$, and we have set here the mean waiting time to be unity. We will also discuss briefly deterministic resetting $\psi_{\text{det}}(\tau) = \delta(\tau - \tau_{\text{det}})$, which is a special case. The second class of PDFs have a power-law tail for large τ ,

$$\psi(\tau) \sim (\tau_0)^\alpha \tau^{-1-\alpha} \quad \text{and} \quad 0 < \alpha < 1. \quad (6)$$

As is well known, these PDFs belong to the domain of attraction of Lévy's laws, and the big jump principle [35] holds instead of standard large deviation theory. In particular, the mean waiting time diverges, and in that sense, the process is scale-free. Other cases like $\alpha = 1$ and $1 < \alpha < 2$ are also of interest, but due to space considerations will not be presented here.

III. STATISTICS OF THE BACKWARD RECURRENCE TIME

In the long-time limit the measurement time t typically falls in a time interval which is longer than the average; see a viewpoint on this issue in [36]. This time interval straddling

time t is a sum of the forward recurrence time (time between t and the first renewal after t) and the mentioned backward time (time between t and the previous reset event). The steady-state (ss) PDF of B for nonlattice PDFs of resetting time is [12,13]

$$f^{\text{ss}}(B) = \frac{1 - \int_0^B \psi(\tau) d\tau}{\langle \tau \rangle}, \quad (7)$$

and $\langle \tau \rangle = \int_0^\infty \tau \psi(\tau) d\tau$ is the mean time between resetting. When $\psi(\tau)$ is exponentially decaying, the distribution of B is $f(B) = \exp(-B)$, and hence is the same as that of the distribution of the time between resetting. More precisely in the long-time limit $f(B, t)$ reaches this steady state, provided that the mean time between resets $\langle \tau \rangle$ is finite (class number one above), and hence

$$\lim_{t \rightarrow \infty} \langle \tau \rangle f(B, t) = 1 - \int_0^B \psi(\tau) d\tau = \mathcal{I}^{\text{ss}}(B). \quad (8)$$

Here we call $\mathcal{I}^{\text{ss}}(B)$ the invariant steady state, which is dimensionless and also a perfectly normalizable function. What happens when $\langle \tau \rangle$ diverges?

If $\alpha < 1$ (class 2), then as shown by Wang *et al.* [14] the PDF of B satisfies

$$\lim_{t \rightarrow \infty} \langle \tau^*(t) \rangle f(B, t) = 1 - \int_0^B \psi(\tau) d\tau = \mathcal{I}^\infty(B). \quad (9)$$

For a brief recap of this and other basic results see Sec. VI. Equation (8) and Eq. (9) appear similar, but they are not. In Eq. (9) $\langle \tau^*(t) \rangle \propto t^{1-\alpha}$ is increasing with measurement time (see below). Still the invariant densities $\mathcal{I}^{\text{ss}}(B)$ and $\mathcal{I}^\infty(B)$ have the same functional dependence on the waiting time PDF, though $\mathcal{I}^\infty(B)$ is called an infinite invariant density since it is not a normalizable function. Since by definition on the left-hand side of Eq. (9) we take a perfectly normalized function $f(B, t)$ and multiply it by a monotonically increasing function of time and take the long-time limit, the integration of $\mathcal{I}^\infty(B)$ over $B > 0$ diverges. This is because $\mathcal{I}^\infty(B) \propto B^{-\alpha}$ and $0 < \alpha < 1$, and hence it is a nonintegrable function due to its large B behavior.

Equations (8) and (9) are valid for any finite B in the limit of long measurement times. However, especially when $0 < \alpha < 1$ the case when B scales with measurement time must also be considered, namely, when $B \propto t$ and t is made large. This limit was studied by Dynkin, who found [12,13]

$$f(B, t) \sim \frac{1}{t} \text{Dyn}\left(\frac{B}{t}\right), \quad (10)$$

and the scaling function reads

$$\text{Dyn}(y) = \frac{\sin \pi \alpha}{\pi} \frac{1}{y^\alpha (1-y)^{1-\alpha}}, \quad 0 < y < 1. \quad (11)$$

This formula shows that the most likely events are obtained when $y \sim 0$ or $y \sim 1$, where the Dynkin PDF diverges, corresponding to either very short B compared to t or B of the order of t . Note that when $\alpha = 1/2$ we find the arcsine law attributed to Lévy.

We see that for $\alpha < 1$ we have two limiting laws, one for B fixed and measurement time long, and the other when the ratio B/t is fixed. The use of these laws, for example, for the calculations of expectation values, depends on the observable

of interest. We will later study observables that are integrable with respect to the infinite density, and show how infinite ergodic theory plays a special role for the nonequilibrium steady states.

Note that Eqs. (9) and (11) are related as they have to match. To see this, using Dynkin's limit theorem, with $B \ll t$ we have

$$f(B, t) \sim \frac{1}{t} \frac{\sin \pi \alpha}{\pi} \frac{1}{(B/t)^\alpha}. \quad (12)$$

On the other hand using Eq. (6), $\mathcal{I}^\infty(B) \sim (\tau_0)^\alpha B^{-\alpha} / \alpha$ for large B . Since $f(B, t) \sim \mathcal{I}^\infty(B) / \langle \tau^*(t) \rangle = (\tau_0)^\alpha B^{-\alpha} / \alpha \langle \tau^*(t) \rangle$ we easily find

$$\langle \tau^*(t) \rangle = \frac{\pi (\tau_0)^\alpha}{\alpha \sin \pi \alpha} t^{1-\alpha}. \quad (13)$$

This is exactly the expression found in [14]. Note that roughly speaking $\langle \tau^*(t) \rangle$ is a mean time between resets, in the sense that if we integrate only up to t $\langle \tau^*(t) \rangle \propto \int^t \tau \psi(\tau) d\tau \sim t^{1-\alpha}$ as indeed we have found. More precisely, let $\langle N \rangle$ be the averaged number of resets in the time interval $(0, t)$. Then in the long-time limit [12]

$$\frac{d\langle N \rangle}{dt} \sim \begin{cases} \frac{1}{\langle \tau^*(t) \rangle} & \text{when } 0 < \alpha < 1 \\ \frac{1}{\langle \tau \rangle} & \text{otherwise.} \end{cases} \quad (14)$$

Thus $1/\langle \tau \rangle$ and $1/\langle \tau^*(t) \rangle$ are the long-time rates of the underlying renewal process; namely $d\langle N \rangle$, which is the probability of observing a reset event in the time interval $(t, t + dt)$, is given by $dt/\langle \tau^*(t) \rangle$ for $0 < \alpha < 1$ and by $dt/\langle \tau \rangle$ otherwise. Thus using Eqs. (8), (9), and (13) we summarize

$$\lim_{t \rightarrow \infty} \frac{f(B, t)}{\left(\frac{d\langle N \rangle}{dt}\right)} = S(B), \quad (15)$$

and $S(B)$ is the survival probability, i.e., the probability of not performing a reset in time B ,

$$S(B) = 1 - \int_0^B \psi(\tau) d\tau = \int_B^\infty \psi(\tau) d\tau. \quad (16)$$

Equation (15) gives the invariant density of the backward time, be it either normalizable or not.

IV. NESS

Using the statistical properties of the backward time we are now ready to explore the density of a packet of particles, in the long-time limit. Different limits must be considered, depending on the existence of the mean time between resetting. We will show that the cases $0 < \alpha < 1$ and $1/2 < \alpha < 1$ must be distinguished.

A. Normalized invariant density

We now consider thin-tailed waiting time PDFs of the first class. The nonequilibrium steady state, $\rho^{\text{ss}}(x)$ is based on the long-time limit of the distribution of B using Eqs. (5), (7), and (16):

$$\lim_{t \rightarrow \infty} \langle \tau \rangle \rho(x, t) = \langle \tau \rangle \rho^{\text{ss}}(x) = \int_0^\infty S(B) \frac{\exp\left(-\frac{x^2}{4DB}\right)}{\sqrt{4\pi DB}} dB. \quad (17)$$

For example, setting $D = 1/2$ and using $\psi(\tau) = \exp(-\tau)$ so $\langle \tau \rangle = 1$ and hence $S(B) = \exp(-B)$ we find the result in [3] $\rho^{\text{ss}}(x) = \exp[-\sqrt{2}|x|]/\sqrt{2}$, which exhibits the typical non-analytical behavior at $|x| \rightarrow 0$. The latter is a rather general feature of NESS, since if we expand the Gaussian in Eq. (17) to second order in x , the x^2 term will diverge, since $S(0) = 1$ and $B^{-3/2}$ is nonintegrable at $B \rightarrow 0$. Pal *et al.* [4] derived a formula for the steady state, which is identical to Eq. (17) without invoking the backward recurrence time and using Laplace transforms (see also [6]). In Appendix A we make the comparison between the two results and explain the different notations. Experimental studies in this regime can be found in [7,37]

B. Scaling solution $0 < \alpha < 1$

Clearly when $\langle \tau \rangle$ diverges we need a different approach. In this case we do not have a steady-state solution; instead, we find for the typical behavior of x a scaling solution that depends on time, and this holds when $x \propto \sqrt{t}$ and both x and \sqrt{t} are large. Inserting Dynkin's limit theorem (10) in Eq. (5) we find

$$\rho(x, t) \sim \frac{1}{t} \int_0^t \text{Dyn}\left(\frac{B}{t}\right) G(x, B) dB. \quad (18)$$

Making this equation explicit, we use Eqs. (1) and (11) and a simple change of variables to obtain

$$\rho(x, t) \sim \frac{g_\alpha(\xi)}{\sqrt{2Dt}} \quad \text{with } \xi = |x|/\sqrt{2Dt}. \quad (19)$$

The scaling here is $x \propto \sqrt{t}$, hence it is diffusive, which is valid for $0 < \alpha < 1$. The scaling function is

$$g_\alpha(\xi) = \frac{\sin \pi \alpha}{\pi} \int_0^1 \frac{\exp\left(-\frac{\xi^2}{2\eta}\right)}{\eta^\alpha (1-\eta)^\alpha} \frac{d\eta}{\sqrt{2\pi\eta}}. \quad (20)$$

This function does not depend on the fine details of the model, i.e., on the waiting time PDF, beyond the parameter α . After a change of variables, we find

$$g_\alpha(\xi) = \frac{1}{\sqrt{2\pi}\Gamma(1-\alpha)} U\left(\alpha, \frac{1}{2} + \alpha, \frac{\xi^2}{2}\right) e^{-\xi^2/2}, \quad (21)$$

where we used the Tricomi function also called the Kummer function of the second kind. This equation was derived with a different approach by Nagar and Gupta [15]. Here we have emphasized the connection between the resetting problem and Dynkin's limit theorem, a worthwhile observation since in many fat-tailed resetting problems, the scaling solution for the stochastic process will depend on this law; for example, if we replace the Gaussian propagator of free diffusion $G(x, B)$ with a propagator of anomalous type, similar laws will follow.

The behavior of the scaling solution in the vicinity of the resetting point $x = 0$ is of interest. Exploiting the small ξ limit

of the Kummer function we have [38]

$$g_\alpha(\xi) \sim \begin{cases} \frac{2^{\alpha-1}}{\sqrt{\pi}} \frac{\Gamma(\alpha-\frac{1}{2})}{\Gamma(1-\alpha)\Gamma(\alpha)} \frac{1}{\xi^{2\alpha-1}} & \frac{1}{2} < \alpha < 1 \\ -\frac{1}{\sqrt{2\pi^{3/2}}} (2 \ln \xi - \gamma - 3 \ln 2) & \alpha = \frac{1}{2} \\ \frac{\Gamma(\frac{1}{2}-\alpha)}{\sqrt{2}\Gamma(1-\alpha)\pi} & 0 < \alpha < \frac{1}{2} \end{cases}, \quad (22)$$

where γ is the Euler-Mascheroni constant. We see that the scaling solution, when $\xi \rightarrow 0$, exhibits a transition at $\alpha = 1/2$. When $0 < \alpha < 1/2$ the scaling function at $x = 0$, namely, $g_\alpha(\xi = 0)$, is a constant, and as Eq. (21) shows this constant diverges when $\alpha \rightarrow 1/2$ from below. Further, when $\alpha \rightarrow 0$ we find $\rho(x = 0, t) \sim g_0(\xi = 0)/\sqrt{2Dt} = 1/\sqrt{4\pi Dt}$, which is the expected result since for $\alpha \rightarrow 0$ the solution $\rho(x, t)$ is the Gaussian PDF describing free BM.

As a stand alone, Eqs. (19) and (22) indicate that $\rho(x, t) \rightarrow \infty$ when $x \rightarrow 0$ (or $\xi \rightarrow 0$) and when $1/2 < \alpha < 1$. Clearly, this is an unphysical effect. The density of the particles $\rho(x, t)$, for thin-tailed distributions on the origin $x = 0$, is always finite for any $t > 0$, and with power-law distributed times between the resetting, we expect an even lower density, since particles can escape to larger distances. We therefore need an alternative approach for this small x limit, which as we show now is described by an infinite invariant density. Roughly speaking, when x is small, the corresponding backward time B is also small, and as we showed, deviations from Dynkin's limit law are present, which will translate into the small x limit of $\rho(x, t)$.

C. Non-normalized invariant density $1/2 < \alpha < 1$

Consider $1/2 < \alpha < 1$ and insert Eq. (9) in Eq. (5) using Eq. (16). We find an expression which looks similar to Eq. (17)

$$\lim_{t \rightarrow \infty} \langle \tau^*(t) \rangle \rho(x, t) = \int_0^\infty S(B) \frac{\exp\left(-\frac{x^2}{4DB}\right)}{\sqrt{4\pi DB}} dB = \tilde{\mathcal{I}}^\infty(x). \quad (23)$$

Of course, the major difference if compared with Eq. (17) is that on the left-hand side of Eq. (23) we have the effective time-dependent mean resetting time $\langle \tau^*(t) \rangle$. The integral converges or diverges if $1/2 < \alpha < 1$ or $0 < \alpha < 1/2$, respectively, and hence here we treat the former case while the latter will be presented soon. The function $\tilde{\mathcal{I}}^\infty(x)$ defined in Eq. (23) is the non-normalizable nonequilibrium steady state of x , as the integration over x of this function diverges. The formula is valid for any finite x in the long-time limit. Note that we use the convention that the argument in the parenthesis defines the infinite density of interest, thus $\mathcal{I}^\infty(B)$ is the infinite density of B while $\tilde{\mathcal{I}}^\infty(x)$ is the infinite density of x . Finally, one can show that the scaling solution and the infinite invariant density match for intermediate x as they should.

D. Non-normalized invariant density $0 < \alpha < 1/2$

What is the infinite density for $0 < \alpha < 1/2$? Using Eq. (19)

$$\lim_{t \rightarrow \infty} \sqrt{2Dt} \rho(x, t) = g_\alpha(0) = \tilde{\mathcal{I}}^\infty(x), \quad (24)$$

and the constant $g_\alpha(0)$ is given in Eq. (22). Here the infinite density is x independent so it is clearly a non-normalizable function, as the integration over x from minus infinity to infinity diverges. The infinite density here does not depend on the structure of the waiting time PDF and, hence, is very different if compared to the invariant densities found for thin-tailed distribution, namely, the normalized state, found in Eq. (23).

E. Plotting

Note that in Eq. (23) we used the ever-increasing timescale $\langle \tau^*(t) \rangle$ to define the non-normalized state, while for the case $0 < \alpha < 1/2$ we used the diverging length scale $\sqrt{2Dt}$. These infinite densities are certainly not probability densities, and their use will be explained later; in fact, the units of the infinite density can be either the inverse of time or inverse of length, depending on the value of α . In general, infinite densities are defined up to some arbitrary constant (since these functions are not normalized we have some freedom in the definition). This does not pose any problem, as long as one recalls the basic definitions. For example, to visualize the infinite density in simulations, we plot the density $\rho(x, t)$ times $\sqrt{2Dt}$ for finite x and increased time, and the solution in the long-time limit will approach $\tilde{\mathcal{I}}^\infty(x)$ for $0 < \alpha < 1/2$. Or we plot $\langle \tau^*(t) \rangle \rho(x, t)$ for a finite range of x , and then as we increase measurement time the solution will approach the asymptotic infinite density (23). Of course, as t is increased, most of the particles are actually diffusing far from the origin. Thus, in practice, if t is too long and the number of trajectories in simulation is not large enough, it will be hard to visualize the infinite densities. To meet this sampling challenge we plot now the non-normalized states for representative cases.

F. Examples

In the examples below we use the Pareto PDF of resetting times,

$$\psi(\tau) = \alpha(t_0)^\alpha \tau^{-(1+\alpha)} \quad \text{for } \tau > t_0. \quad (25)$$

In this case

$$\langle \tau^*(t) \rangle \sim (\pi / \sin \pi \alpha) t^{1-\alpha}, \quad (26)$$

where we used Eqs. (6) and (13) and we set $t_0 = 1$ and $D = 1/2$. It follows from Eq. (23)

$$\tilde{\mathcal{I}}^\infty(x) = \int_0^1 \frac{\exp(-\frac{x^2}{2B})}{\sqrt{2\pi B}} dB + \int_1^\infty B^{-\alpha} \frac{\exp(-\frac{x^2}{2B})}{\sqrt{2\pi B}} dB. \quad (27)$$

For $x = 0$ we find

$$\tilde{\mathcal{I}}^\infty(0) = \sqrt{\frac{2}{\pi}} \frac{\alpha}{\alpha - \frac{1}{2}}. \quad (28)$$

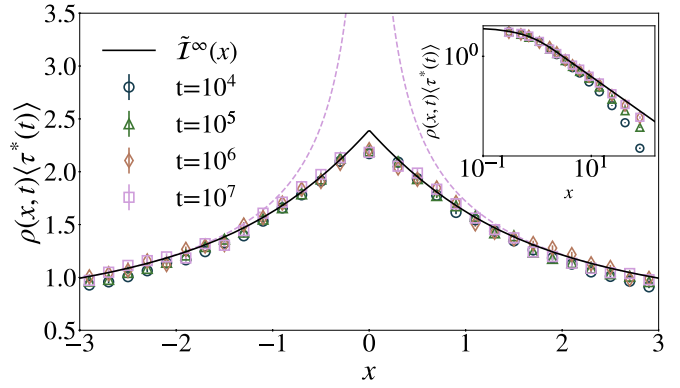


FIG. 2. The infinite density vs x for $\alpha = 3/4$. From simulations, we plot the histogram for the density $\rho(x, t)$ multiplied by $\langle \tau^*(t) \rangle$ vs x . Increasing time we see that results converge to the theoretical prediction, namely, the solid line presenting the infinite density $\tilde{\mathcal{I}}^\infty(x)$, Eq. (30). For large x , $\tilde{\mathcal{I}}^\infty(x) \simeq 1/|x|^{1/2}$, Eq. (31), hence this invariant density is not normalized. The infinite density exhibits a typical cusp on the origin. Also shown is the scaling solution (22) for time 10^7 (dashed line). The latter is a good approximation for diffusive scales, namely, when x of the order $t^{1/2}$, but for small x presented here, the scaling solution clearly fails. We use the Pareto PDF of times between resets with $t_0 = 1$ and $D = 1/2$. We have used 1.3×10^6 trajectories. Inset: We present the large x , and the data for various times do not collapse on a master curve, unlike the small x shown in the main figure.

Hence for $1/2 < \alpha < 1$ the density on the origin

$$\rho(0, t) \sim \frac{\tilde{\mathcal{I}}^\infty(0)}{\langle \tau^*(t) \rangle} \quad (29)$$

is decreasing with time, and the divergence of the scaling solution (22) at $\xi = x = 0$ is not relevant, since as mentioned that solution is not valid in this regime. For the example, $\alpha = 3/4$ Eq. (27) gives

$$\tilde{\mathcal{I}}_{\alpha=3/4}^\infty(x) = |x| \left[\operatorname{erf}\left(\frac{|x|}{\sqrt{2}}\right) - 1 \right] + \sqrt{\frac{2}{\pi}} e^{-\frac{x^2}{2}} + \frac{\Gamma(\frac{1}{4}) - \Gamma(\frac{1}{4}, \frac{x^2}{2})}{2^{1/4} \sqrt{\pi} \sqrt{|x|}}, \quad (30)$$

where we use the error function and the incomplete Gamma function. This invariant density is plotted in Fig. 2 together with finite-time numerical simulations. As shown the infinite density exhibits a cusp on the resetting point $x = 0$, which is found also for resetting problems with a normalized invariant density. For large x we have

$$\tilde{\mathcal{I}}_{\alpha=3/4}^\infty(x) \sim \frac{\Gamma(\frac{1}{4})}{2^{1/4} \sqrt{\pi} \sqrt{|x|}}. \quad (31)$$

This expression can be shown to match the small x behavior of the scaling solution (22). Similarly, in Fig. 3 we study the case $\alpha = 1/4$. As predicted by theory the infinite density is structureless, namely, it is equal to a constant. This is clearly unlike what we see in Fig. 2, so the transition at $\alpha = 1/2$ is evident.

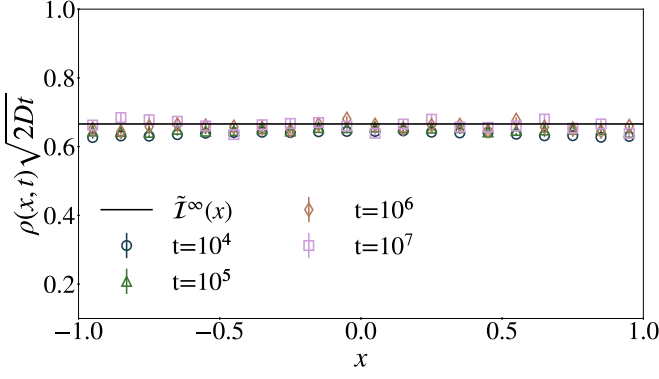


FIG. 3. The infinite density vs x for $\alpha = 1/4$. From simulations, we plot the histogram for the probability density $\rho(x, t)$ multiplied by $\sqrt{2Dt}$, unlike the case $\alpha > 1/2$ where we use $\langle \tau^*(t) \rangle$, as shown in Fig. 2. The solid line is the theory, the infinite density $\tilde{T}^\infty(x)$ (24), namely, $\tilde{T}_{1/4}(x) = g_{1/4}(0) = \Gamma(1/4)/\sqrt{2}\Gamma(3/4)\pi \simeq 0.6659$. Now the infinite density is simply a constant, and the cusp found for $\alpha = 3/4$ in Fig. 2 is not present. Further, clearly a constant invariant density is not normalized. We use the Pareto PDF of times between resets with $t_0 = 1$ and $D = 1/2$. We have used 10^8 trajectories.

V. THE MOMENTS

Moments of stochastic processes are used extensively to characterize data and hence will be studied here as well. In the context of infinite ergodic theory, one treats two classes of observables: those that are integrable with respect to the infinite density and those that are not. The basic issue is that we have for $0 < \alpha < 1$ two limiting laws, the infinite densities and the scaling solution. As shown in this work some of the statistical averages are calculated based on the former and some with respect to the latter. This classification of observables is also important when the ergodic theory is considered.

A. Thin-tailed distributions

Using Eq. (2) the moments of the process satisfy

$$\langle x^{2m}(t) \rangle = D^m \langle \xi^{2m} \rangle \langle B^m \rangle, \quad (32)$$

and here $m = 0, 1, 2, \dots$. We used the fact that odd moments of $x(t)$ vanish from symmetry. Recall that the PDF of ξ is Gaussian with zero mean and variance equal to 2, PDF(ξ) = $\exp(-\xi^2/4)/\sqrt{4\pi}$. In the normalized steady state, when we deal with thin-tailed PDFs of resetting times, the moments of B become time-independent and so do the moments of $x(t)$. For example,

$$\langle x^2 \rangle_{ss} = 2D \langle B \rangle_{ss}. \quad (33)$$

and in general $\langle x^{2m} \rangle_{ss} = D^m \langle \xi^{2m} \rangle \langle B^m \rangle_{ss}$, where

$$\langle \xi^{2m} \rangle = \frac{4^m \Gamma(m + 1/2)}{\sqrt{\pi}}. \quad (34)$$

In turn, the moments of B are determined by the moments of $\psi(\tau)$ using Eq. (7). We use the Laplace transform $\hat{\psi}(s) = \int_0^\infty \exp(-s\tau)\psi(\tau)d\tau$, and similarly $\hat{f}_{ssB}(s)$ is the Laplace pair of $f_{ss}(B)$. Using the convolution theorem and Eq. (7),

$$\hat{f}_{ssB}(s) = \frac{1 - \hat{\psi}(s)}{s\langle \tau \rangle}. \quad (35)$$

The Laplace transforms are also moment-generating functions; hence expanding for small s ,

$$\hat{\psi}(s) = 1 - s\langle \tau \rangle + s^2 \frac{\langle \tau^2 \rangle}{2} + \dots, \quad (36)$$

where $\langle \tau^m \rangle$ are the moments of the times between resets and similarly

$$\hat{f}_{ssB}(s) = 1 - s\langle B \rangle_{ss} + s^2 \frac{\langle B^2 \rangle_{ss}}{2} + \dots. \quad (37)$$

Inserting Eqs. (36) and (37) in Eq. (35) we find

$$\begin{aligned} 1 - s\langle B \rangle_{ss} + s^2 \frac{\langle B^2 \rangle_{ss}}{2} + \dots \\ = \frac{1 - \left(1 - s\langle \tau \rangle + s^2 \frac{\langle \tau^2 \rangle}{2} - \frac{s^3 \langle \tau^3 \rangle}{3!} + \dots\right)}{s\langle \tau \rangle}. \end{aligned} \quad (38)$$

Comparing terms of the same order we have $\langle B \rangle_{ss} = \langle \tau^2 \rangle / (2\langle \tau \rangle)$, $\langle B^2 \rangle_{ss} = \langle \tau^3 \rangle / (3\langle \tau \rangle)$, and in general $\langle B^m \rangle_{ss} = \langle \tau^{m+1} \rangle / [(m+1)\langle \tau \rangle]$. From Eq. (32) we find

$$\langle x^2 \rangle_{ss} = D \frac{\langle \tau^2 \rangle}{\langle \tau \rangle} \quad (39)$$

and more generally

$$\langle x^{2m} \rangle_{ss} = \frac{4^m}{(m+1)} \frac{\Gamma(m + \frac{1}{2})}{\sqrt{\pi}} \frac{D^m \langle \tau^{m+1} \rangle}{\langle \tau \rangle}. \quad (40)$$

B. Fat-tailed distributions

Equation (32) is still valid when $0 < \alpha < 1$. Noticing that B^m is nonintegrable with respect to the infinite density (9), since the latter decays like $B^{-\alpha}$ for large B , we realize that the moments are determined by the large x behavior of the propagator $\rho(x, t)$, when the scaling presented in Eq. (21) is diffusive. One may in principle find the moments $\langle x^{2m}(t) \rangle$ using the properties of the Kummer function; however, there is no need for that. Equation (32) is still valid, and the moments increase with time, for example,

$$\langle x^2(t) \rangle \sim 2D \langle B(t) \rangle_{\text{Dyn}}. \quad (41)$$

In turn, the moments of the backward recurrence time are obtained using Dynkin's limiting law [Eqs. (10) and (11)]. For $m = 0, 1, \dots$ we use

$$\int_0^1 \frac{y^{m-\alpha}}{(1-y)^{1-\alpha}} dy = \frac{\Gamma(\alpha)\Gamma(m-\alpha+1)}{m!}, \quad (42)$$

and hence

$$\langle B^m(t) \rangle_{\text{Dyn}} \sim \frac{\Gamma(m-\alpha+1)}{m!\Gamma(1-\alpha)} t^m. \quad (43)$$

Then we find the diffusive type of scaling for the moments,

$$\langle x^{2m}(t) \rangle \sim D^m \langle \xi^{2m} \rangle \langle B^m(t) \rangle_{\text{Dyn}}, \quad (44)$$

which is made explicit with Eqs. (34) and (43). In the limit $\alpha \ll 1$ we have $\langle B^m(t) \rangle_{\text{Dyn}} \sim t^m$ since then the resetting is extremely sparse, and as expected the moments $\langle x^{2m}(t) \rangle$ are determined by free diffusion.

We see that the moments of the process are determined by the scaling solution of B Eq. (10), and hence are not sensitive

to the details of the waiting time PDF $\psi(\tau)$. This is because the moments explore the large x part of the density $\rho(x, t)$. Observables of another class, considered in the next section, are integrable with respect to the non-normalized state. These do not exhibit diffusive scaling, and their ergodic properties are of special interest as they are related to the non-normalized NESS found here.

VI. FRACTIONAL INTEGRAL EQUATION FOR THE DENSITY

The goal of this section is to find a valid approximation for $\rho(x, t)$ in the limit of long times; this should hold both for large and small x . As we showed, the infinite density approach works well for small x , and the scaling solution works well for large x , so now we want to marry the two solutions, using a uniform approximation. Further, close to the transition $\alpha = 1/2$ the convergence to asymptotic results is extremely slow, and this can be overcome with the uniform approximation.

We focus on fat-tailed PDFs of waiting time (6), $\psi(\tau) \sim (\tau_0)^\alpha \tau^{-1-\alpha}$, and $0 < \alpha < 1$. As usual, we will use the Laplace transform of this function, for small s [9,12,39],

$$\hat{\psi}(s) \sim 1 - b_\alpha s^\alpha + \dots, \quad \text{where } b_\alpha = (\tau_0)^\alpha \frac{\Gamma(1-\alpha)}{\alpha}. \tag{45}$$

We start with a recap of a handful of known results from the field of renewal processes [12,14,40] which are used in this study. Our goal is to find an improved approximation for the statistics of the backward time, with which we can find the sought-after uniform approximation for $\rho(x, t)$. This will lead to an interesting connection between the resetting problem and fractional calculus.

A. Statistics of number of jumps

Let $P_t(N)$ be the probability for N renewals in the period $(0, t)$. Using the convolution theorem of Laplace transform

$$\hat{P}_s(N) = \frac{1 - \hat{\psi}(s)}{s} [\hat{\psi}(s)]^N, \tag{46}$$

where $\hat{P}_s(N)$ is the Laplace $t \rightarrow s$ transform of $P_t(N)$. The mean number of jumps is $\langle N(t) \rangle$, and its Laplace pair reads [60]

$$\langle \hat{N}(s) \rangle = \sum_{N=0}^{\infty} N \hat{P}_s(N) = \frac{\hat{\psi}(s)}{s[1 - \hat{\psi}(s)]}. \tag{47}$$

Inserting Eq. (45) and inverting to the time domain

$$\langle N(t) \rangle \sim \frac{\sin \pi \alpha}{\pi} \left(\frac{t}{\tau_0} \right)^\alpha, \tag{48}$$

where we used the reflection formula for the Γ function. Equation (48) obeys (14).

B. Backward time statistics

A technique for finding the distribution of the backward recurrence time is given in [12], and it is based on double Laplace transforms. Let $f_B(t, B)$ be the PDF of B and

$\hat{f}_B(s, u) = \int_0^\infty dt \int_0^\infty dt \exp(-st - uB) f_B(t, B)$. Without any approximation

$$\hat{f}_B(s, u) = \frac{1 - \hat{\psi}(s+u)}{s+u} \frac{1}{1 - \hat{\psi}(s)}. \tag{49}$$

Here $\hat{\psi}(s+u) = \int_0^\infty \exp[-(s+u)\tau] \psi(\tau) d\tau$. In principle, if we can invert this formula to the double time domain, i.e., t and B , we can find $\rho(x, t)$ using Eq. (5). Using Eq. (45), in the limit when $s \rightarrow 0$ and $u \rightarrow 0$ their ratio remaining finite,

$$\hat{f}_B(s, u) \sim s^{-\alpha} (s+u)^{\alpha-1}. \tag{50}$$

This equation is independent of the fine details of the waiting time PDF besides α . The inversion to the time domain is carried out in [12] yielding Dynkin's limit theorem [Eqs. (10) and (11)]. If the mean waiting time is finite, one uses Eq. (49) to find Eq. (8). Technically this is done by considering the limit $s \rightarrow 0$ while leaving u fixed, which in turn, upon Laplace inversion, gives the long-time limit of the problem.

Switching back to $0 < \alpha < 1$ such that the mean waiting time diverges, we consider Eq. (49) in the limit $s \rightarrow 0$ and u finite [14]. Using Eq. (45),

$$\hat{f}_B(s, u) \sim \frac{1 - \hat{\psi}(u)}{u} \frac{1}{b_\alpha s^\alpha}. \tag{51}$$

Inverting to the (t, B) domain one finds Eq. (9). This describes the statistics of finite B when t is made large.

C. Example $\alpha = 1/2$

To demonstrate this behavior we consider an example. Let

$$\psi(\tau) = \frac{\exp(-\frac{1}{2\tau})}{\sqrt{2\pi} \tau^{3/2}}; \tag{52}$$

hence $\alpha = 1/2$. This PDF is called the one-sided Lévy stable distribution with index $1/2$, and is known as a van der Waals profile. In this case $\sqrt{\tau_0} = \sqrt{2/\pi}$ and $\langle \tau^*(t) \rangle = \sqrt{2\pi} t^{1/2}$. Using Eq. (9) we find

$$\lim_{t \rightarrow \infty} \langle \tau^*(t) \rangle f(B, t) = \text{Erf} \left(\frac{1}{\sqrt{2B}} \right), \tag{53}$$

where we introduce the error function. Recall that $\text{Erf}(1/\sqrt{2B}) \sim 1$ for $B \rightarrow 0$ and $\text{Erf}(1/\sqrt{2B}) \sim \sqrt{2/\pi} B^{-1/2}$ for large B . Hence the B integration of this infinite invariant density diverges $\int_0^\infty \text{Erf}(1/\sqrt{2B}) dB = \infty$, due to the large B limit.

We now consider finite-time simulations to demonstrate the result. Generating the sequence of waiting times we find the statistics of B using 10^7 samples. The random waiting times are given by $\tau = 1/G^2$, where G is a Gaussian random variable with zero mean, whose PDF is $\exp[-G^2/2]/\sqrt{2\pi}$ [42]. Generating such a normally distributed random variable with a computer program is a standard routine. Hence it is easy to generate the realizations of the renewal sequence and sample the random variable B on a computer.

In Fig. 4 we plot the typical fluctuations of B which are captured by Dynkin's limit theorem' in fact, since $\alpha = 1/2$ we find the arcsine law. To do so we plot the histogram of the random variable B/t , which is clearly bounded in the unit interval. One sees the well-known U shaped histogram, meaning

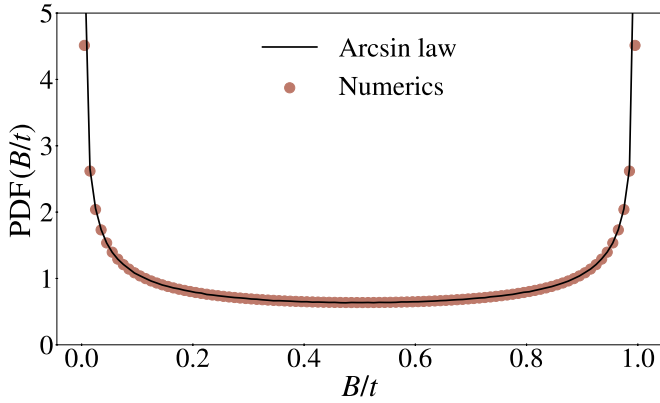


FIG. 4. Numerical simulations for the PDF of the rescaled backward recurrence time $0 < B/t < 1$ for $\alpha = 1/2$ converge to the arcsine law. Deviations from this well-known behavior are presented in Fig. 5.

that small B and large B are by far more likely if compared to the mean which in the long-time limit is $\langle B/t \rangle = 1/2$. Small deviations from the asymptotic theory are observed on the left, and those are rare events.

To study these we focus on $0 < B < 3 \ll t$. Here the infinite density is a valid approximation while the arcsine law is clearly invalid. In Fig. 5 we plot the normalized histogram for the backward time, namely, the sample estimation of the PDF of B , multiplied by $\langle \tau^*(t) \rangle$ vs B . The numerical result matches $\text{Erf}(1/\sqrt{2B})$ without any fitting, indicating that also for finite-time simulations the non-normalized result is a good approximation.

D. Uniform approximation for B

We have considered already the PDF of B , $f_B(B, t)$ in two limits. The typical behavior (10), when B is scaled with time t

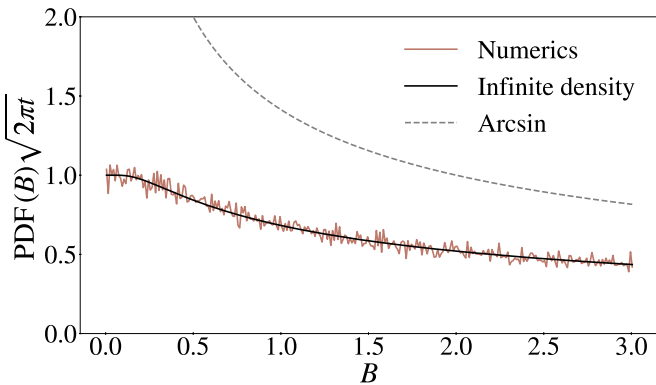


FIG. 5. Numerical simulations for the PDF of the backward recurrence time B , multiplied by $\langle \tau^*(t) \rangle$, perfectly match the prediction based on the infinite invariant density (53). Note that $0 < B < 3$ while $t = 10^4$, hence the figure presents the small B behavior of the density. Here $\alpha = 1/2$, hence the arcsine law (11) describes the typical fluctuations of B ; however, as shown and as expected it fails here (it works fine in the large B regime). As a stand alone the arcsine law predicts that the density will diverge when $B \rightarrow 0$, which is clearly not the case for any finite t . In simulations, we use 10^7 realizations of the renewal process. The PDF of waiting times is given in Eq. (52); hence $\langle \tau^*(t) \rangle = \sqrt{2\pi t}$.

and the rare events (9). An important scale of $\psi(\tau)$, is roughly speaking the time beyond which $\psi(\tau) \sim (\tau_0)^\alpha \tau^{-1-\alpha}$ is a valid approximation. For the Pareto distribution (25) this timescale is t_0 , while for the one-sided Lévy stable law (52) it is of order unity. For B larger than this timescale the two solutions match, as mentioned already.

Now we present a simple uniform approximation for the density of B :

$$f_{\text{Uni}}(B, t) = \begin{cases} \frac{S(B)}{\langle \tau^*(t-B) \rangle} & 0 < B < t \\ 0 & \text{otherwise} \end{cases}. \quad (54)$$

This is obtained by matching the two solutions mentioned above. Equation (54) holds for large t . By construction, for large B , we have $S(B) \sim (\tau_0/B)^\alpha/\alpha$, and hence this solution matches Dynkin's limit theorem (10), while for small B it yields Eq. (15). We find the uniform approximation for the density of reset particles. Using Eqs. (5) and (54),

$$\rho_{\text{Uni}}(x, t) = \int_0^t dB \frac{S(B)G(x, B)}{\langle \tau^*(t-B) \rangle}. \quad (55)$$

This is one of the main results of the paper as it provides both the large x limit of the density $\rho(x, t)$ (described also by the scaling solution) and the small x limit (given by the infinite density). Employing Eq. (13) for $\langle \tau^*(t) \rangle$ and the definition of the left-sided fractional Riemann-Liouville integration,

$${}_0D_t^{-\alpha} g(t) = \frac{1}{\Gamma(\alpha)} \int_0^t g(t')(t-t')^{\alpha-1} dt', \quad (56)$$

we find

$$(\tau_0)^\alpha |\Gamma(-\alpha)| \rho_{\text{Uni}}(x, t) = {}_0D_t^{-\alpha} [S(t)G(x, t)]. \quad (57)$$

This equation holds far beyond the case of Brownian motion. It connects the survival probability, the propagator for reset free motion, and the density of the spreading particles. It describes both the small x limit which is dominated by small B statistics as well as the scaling solution to the problem, discussed previously. Note that the inverse operation of the fractional integration is a fractional derivative; hence we may use Marchaut's formula to find, at least in principle, the product $S(t)G(x, t)$, from the density of an ensemble of particles undergoing the resetting process.

E. The transition case $\alpha = 1/2$

Using $\alpha = 1/2$ as an example and for the waiting time PDF (52) we have from Eq. (16) the survival probability $S(B) = \text{Erf}(1/\sqrt{2B})$, and $\langle \tau^*(t) \rangle = \sqrt{2\pi t}$, as mentioned. Therefore the uniform approximation reads

$$\rho_{\text{Uni}}(x, t) = \int_0^t dB \frac{\text{Erf}\left(\frac{1}{\sqrt{2B}}\right)G(x, B)}{\sqrt{2\pi(t-B)}}, \quad (58)$$

where we used $D = 1/2$. This for large x describes well the typical fluctuations given by the arcsine law for B ,

$$\rho_{\text{Arcsine}}(x, t) = \int_0^t dB \frac{G(x, B)}{\pi \sqrt{B} \sqrt{t-B}}, \quad (59)$$

which is the same as Eq. (18) for $\alpha = 1/2$. This approximation diverges on the origin $x = 0$ namely, in the vicinity of the resetting point, while in reality and according to Eq. (58) such

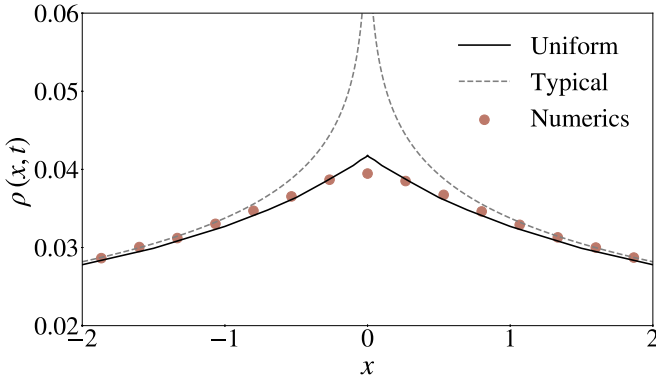


FIG. 6. Numerics for the PDF of the position x for an ensemble of particles undergoing the resetting process with $\alpha = 1/2$. We focus on the small x behavior, namely, the vicinity of the resetting point $x = 0$. The uniform approximation (58) perfectly matches the simulations, while the scaling solution (59) describing the typical fluctuations (large x) fails. Here $t = 10^3$, the resetting time PDF is Eq. (52), and we used 10^7 realizations.

behavior is not found. The two solutions are used in Fig. 6, where the numerics clearly demonstrates that the uniform approximation is the valid theory. Both the uniform solution and numerics exhibit a cusp in the density close to $x = 0$.

Using Eq. (58) we obtain the probability of finding the particles in the interval $(-1, 1)$. We use $\int_{-1}^1 \exp[-x^2/(2B)] dx/\sqrt{2\pi B} = \text{Erf}[1/\sqrt{2B}]$ to find

$$\text{Prob}_{\text{Uni}}(-1 < x < 1) = \frac{1}{\sqrt{2\pi}} \int_0^t \frac{\text{Erf}^2\left[\frac{1}{\sqrt{2B}}\right]}{\sqrt{t-B}} dB. \quad (60)$$

This integral is solved numerically and compared with Monte Carlo simulations in Fig. 7 showing the validity of the uniform approximation. We compare this solution to the one obtained using the description of the typical fluctuations, namely, using the scaling function $g_\alpha(\xi)$ with $\alpha = 1/2$. Recall that this solution does not depend explicitly on the waiting time PDF $\psi(\tau)$

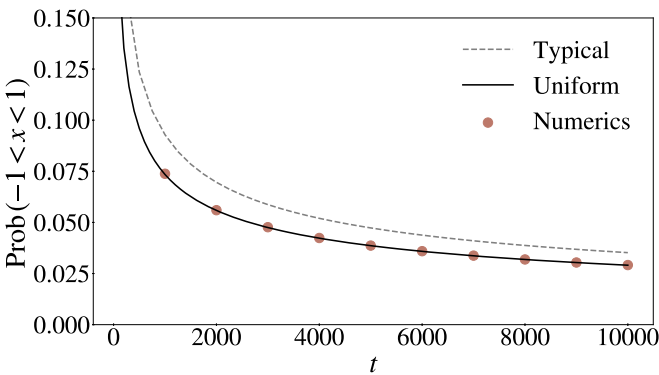


FIG. 7. Probability of occupying the interval $-1 < x < 1$ for a resetting process to the origin $x = 0$ vs time. Here we use the one-sided Lévy distribution (52) to model the time intervals between resetting, so $\alpha = 1/2$, which is the transition exponent. Simulations nicely match the uniform approximation (60), while the theory based on typical fluctuations (61) does not work so well. Here $D = 1/2$ and for simulations we use 2×10^7 trajectories.

besides α of course, unlike the uniform approximation. Using Eq. (22) and $D = 1/2$,

$$\begin{aligned} \text{Prob}_{\text{typical}}(-1 < x < 1) &\simeq - \int_{-1}^1 dx \frac{1}{\sqrt{2t\pi^{3/2}}} [2 \ln |x|/\sqrt{t} - \gamma - 3 \ln 2] \\ &= \frac{\sqrt{2}}{\sqrt{t\pi^3}} (\ln t + 2 + \gamma + 3 \ln 2). \end{aligned} \quad (61)$$

This solution is plotted in Fig. 7 where its performance compared with the uniform approximations is shown to be weak. The $\ln(t)$ logarithmic behavior in (61) indicates the particularly slow nature of convergence to asymptotic results, strengthening the need for the uniform approximation at this transition case $\alpha = 1/2$. We also integrated Eq. (59) in the interval $-1 < x < 1$ to estimate $\text{Prob}(-1 < x < 1)$. This solution works slightly better than the simple analytical expression Eq. (61) yet still not matching the uniform approximation (60). It is not plotted to avoid burdening the eye.

F. Uniform approximation: An example

We now check the predictions of the uniform approximation using the Pareto distribution for waiting times and $\alpha = 1/4$ so $\psi(\tau) = 0.25\tau^{-5/4}$ for $\tau > 1$, otherwise $\psi(\tau) = 0$. In this case, from Eq. (6), $(\tau_0)^{1/4} = 1/4$, and using Eq. (13) $\langle \tau^*(t) \rangle = \sqrt{2\pi t^{3/4}}$. The survival probability is $S(B) = 1$ if $B < 1$ and $S(B) = B^{-1/4}$ for $1 < B$; hence, using Eq. (55), we have for $t > 1$

$$\rho_{\text{Uni}}(x, t) = \int_0^1 \frac{G(x, B) dB}{\sqrt{2\pi}(t-B)^{3/4}} + \int_1^t \frac{G(x, B) dB}{\sqrt{2\pi}B^{1/4}(t-B)^{3/4}}. \quad (62)$$

This solution should be compared with the one obtained using the scaling solution (18),

$$\rho(x, t) \sim \frac{1}{\sqrt{2\pi}} \int_0^t \frac{G(x, B) dB}{(t-B)^{3/4}B^{1/4}}, \quad (63)$$

which is valid when x and t are large while $\xi = |x|/\sqrt{t}$ is finite and we set $D = 1/2$. This gives according to Eq. (19) $\rho(x, t) \sim g_{1/4}(\xi)/\sqrt{t}$ where the scaling function $g_{1/4}(\xi)$ is presented in Eq. (21). Recall that from the infinite density (24) we have the approximation, valid for finite x and large t ,

$$\rho(x, t) \sim \frac{g_{1/4}(0)}{\sqrt{2Dt}} = \frac{\Gamma(1/4)\sqrt{t}}{\sqrt{2}\Gamma(3/4)\pi} \simeq \frac{0.66593}{\sqrt{t}}. \quad (64)$$

In Fig. 8 we make the comparison between the various approximations. The figure shows that for finite time t , the uniform approximation works very well. Of course, for the very long-time limit the simulation results will converge to the theoretical prediction of the infinite density, which is given by the straight line in the figure.

We also find the probability that the particle is in the interval $-1 < x < 1$ at time t . Using $\int_{-1}^1 G(x, B) dx = \text{Erf}[1/\sqrt{2B}]$ we have for the uniform approximation

$$\begin{aligned} \text{Prob}_{\text{Uni}}(-1 < x < 1) &= \int_0^1 \frac{\text{Erf}\left[\frac{1}{\sqrt{2B}}\right] dB}{\sqrt{2\pi}(t-B)^{3/4}} + \int_1^t \frac{\text{Erf}\left[\frac{1}{\sqrt{2B}}\right] dB}{\sqrt{2\pi}(t-B)^{3/4}B^{1/4}}. \end{aligned} \quad (65)$$

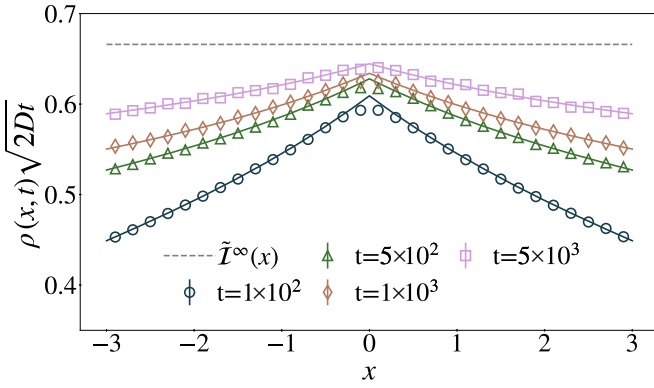


FIG. 8. Infinite density vs x for using the Pareto PDF for waiting times with $\alpha = 1/4$ and $t_0 = 1$. In simulation we plot the histogram for the probability density $\rho(x, t)$ multiplied by $\sqrt{2Dt}$. In solid lines the uniform approximation (62) for intermediate times, and in dashed lines the infinite density $\tilde{L}^\infty(x) \simeq 0.6659$, Eq. (24). Here $D = 1/2$ and we use 10^8 trajectories.

These integrals can be numerically computed using programs like *Mathematica* or *Maple*. On the other hand from Eq. (64) we have

$$\text{Prob}(-1 < x < 1) \simeq 0.66592 |\Delta x| / \sqrt{t},$$

where $|\Delta x| = 2$ is the length of the interval $-1 < x < 1$ under study.

Figure 9 clearly demonstrated the useful aspect of the uniform approximation as it captures the approach to the asymptotic limit, i.e., the straight line in the figure.

VII. THE SPECIALNESS OF SHARP RESTART

We will soon study the ergodic properties of the process, with emphasis on fat-tailed resetting processes. Before doing so we comment on a thin-tailed case, the well-studied sharp restart.

A natural question is to what extent can we squeeze the steady state distribution of x ? Of course, fast resetting will simply put the particle always on the origin. If we fix $\langle \tau \rangle$

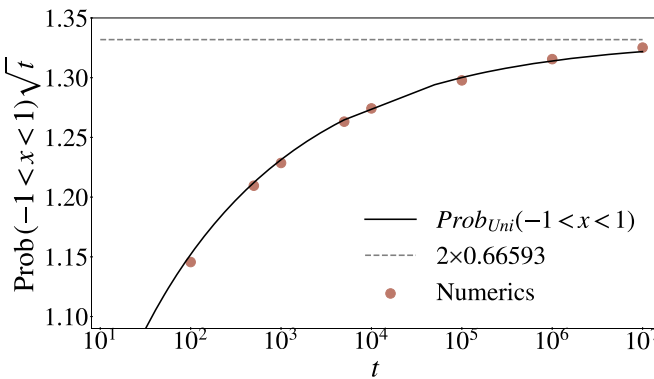


FIG. 9. Probability of occupying the interval $-1 < x < 1$ times \sqrt{t} as a function of time. The points belong to the data from Fig. 3 and Fig. 8, while the solid line represents the uniform approximation (65). Times between resets follow a Pareto PDF with $t_0 = 1$, $\alpha = 1/4$. D is $1/2$, and we use 10^8 realizations.

to some nonzero value, the narrowest steady state PDF of x will be naively found when $\psi(\tau) = \delta(\tau - \langle \tau \rangle)$. This strategy is called sharp restart, and its NESS was studied in [6]. Further, sharp restart is optimal for search [43,44] and hence studied extensively [45]. In this case, the variance of x is $\langle x^2 \rangle_{ss} = D\langle \tau \rangle$, which is smaller than any other $\langle x^2 \rangle_{ss}$ [given by Eq. (39)] found with another choice of $\psi(\tau)$, since in general $\langle \tau^2 \rangle / \langle \tau \rangle \geq \langle \tau \rangle$ and hence sharp restart gives the minimum of the dispersion.

However, sharp restart implies the nonexistence of NESS. To see this note that at any time t is slightly larger than an integer times $\langle \tau \rangle$, the particle is on $x \simeq 0$. In contrast just before these times, the PDF of x is a Gaussian with variance, $2D\langle \tau \rangle$. In short, for stroboscopic resetting, which starts at time $t = 0$, we have no NESS, in the sense that the PDF of x is time-dependent, with a periodicity which is the sharp time between resets. One can claim that if the restart is nearly sharp, i.e., if we have a narrow but analytical PDF of $\psi(\tau)$ around some $\langle \tau \rangle$, namely, some small uncertainty in the resetting times, the process will converge to the NESS. While this is correct, this convergence will take very long, and the narrower the PDF of reset times, around the sharp reset time $\langle \tau \rangle$, the longer the relaxation towards the NESS will be. Another option for obtaining a NESS, for lattice PDFs of resetting time, is to randomize the initial clock; however, this option is not part of this work.

VIII. ERGODIC THEORY

So far we have studied useful approximations for the density of particles. We now study the ergodic properties of the process. Consider an observable, namely, a functional of the stochastic path of the resetting process, $\mathcal{O}[x(t)]$ [46,47]. The time averages are denoted by

$$\overline{\mathcal{O}(t)} = \frac{1}{t} \int_0^t \mathcal{O}[x(t')] dt', \quad (66)$$

while the ensemble average is $\langle \mathcal{O}(t) \rangle = \int_{-\infty}^{\infty} \mathcal{O}(x) \rho(x, t) dx$. For thin-tailed PDFs of resetting times, excluding sharp restart, the time and ensemble averages are identical in the long-time limit

$$\lim_{t \rightarrow \infty} \overline{\mathcal{O}(t)} = \langle \mathcal{O} \rangle^{ss} \quad (67)$$

and

$$\langle \mathcal{O} \rangle^{ss} = \int_{-\infty}^{\infty} \mathcal{O}(x) \rho^{ss}(x) dx, \quad (68)$$

where the normalized NESS density $\rho^{ss}(x)$ is defined in Eq. (17). We did not prove this expected result, but some arguments as to why it is correct are given below. Note that in Eq. (68) we have assumed that the integral on the right-hand side does not diverge, namely, that the observable $\mathcal{O}(x)$ is integrable with respect to the normalized steady state. So far in this section $\langle \tau \rangle$ was finite; what is the ergodic theory when this mean time diverges?

For fat-tailed resetting times, with $0 < \alpha < 1$ infinite ergodic theory holds. This means that the non-normalized steady state will play a special role in the evaluation of the time averages. First, consider the ensemble averages: in the

long-time limit we find two types of behaviors. For $1/2 < \alpha < 1$ using Eq. (23),

$$\langle \mathcal{O}(t) \rangle = \int_{-\infty}^{\infty} \mathcal{O}(x) \rho(x, t) dx \sim \frac{\int_{-\infty}^{\infty} \mathcal{O}(x) \tilde{\mathcal{I}}^{\infty}(x) dx}{\langle \tau^*(t) \rangle}, \quad (69)$$

where we use Eq. (23), so $\rho(x, t) \sim \tilde{\mathcal{I}}^{\infty}(x) / \langle \tau^*(t) \rangle$. Similarly using Eq. (24) for $0 < \alpha < 1/2$,

$$\langle \mathcal{O}(t) \rangle \sim \frac{\int_{-\infty}^{\infty} \mathcal{O}(x) \tilde{\mathcal{I}}^{\infty}(x) dx}{\sqrt{2Dt}}. \quad (70)$$

We have assumed that the integrals do not diverge, namely, that the observable is integrable with respect to the infinite invariant density $\tilde{\mathcal{I}}^{\infty}(x)$. Equations (69) and (70) show that while $\tilde{\mathcal{I}}^{\infty}(x)$ is not normalized, it is used to obtain ensemble averages. More precisely

$$\begin{aligned} \lim_{t \rightarrow \infty} \langle \tau^*(t) \rangle \langle \mathcal{O}(t) \rangle &= \int_{-\infty}^{\infty} \mathcal{O}(x) \tilde{\mathcal{I}}^{\infty}(x) dx \quad \text{if } 1/2 < \alpha < 1, \\ \lim_{t \rightarrow \infty} \sqrt{2Dt} \langle \mathcal{O}(t) \rangle &= \int_{-\infty}^{\infty} \mathcal{O}(x) \tilde{\mathcal{I}}^{\infty}(x) dx \quad \text{if } 0 < \alpha < 1/2; \end{aligned} \quad (71)$$

thus $\langle \tau^*(t) \rangle$ and $\sqrt{2Dt}$ replace normalizing factors.

As an example of an integrable observable consider

$$\mathcal{O}[x(t)] = \theta(a < x(t) < b), \quad (72)$$

where $\theta(a < x(t) < b)$ is the pulse function; namely, it is equal unity if the condition in the parentheses holds, otherwise it is zero. Since the integral $\int_a^b \tilde{\mathcal{I}}^{\infty}(x) dx$ is finite, for finite a and b , the observable is called integrable, and we will now use this observable to discuss time averages.

A. Example

As an example consider the case $\alpha = 3/4$ with the Pareto PDF discussed in Sec. IV F with $D = 1/2$. The observable of interest is the pulse function $\theta[-3 < x(t) < 3]$. Using the infinite density (30),

$$\langle \tau^*(t) \rangle \langle \theta[-3 < x(t) < 3] \rangle \sim \int_{-3}^3 \tilde{\mathcal{I}}_{\alpha=3/4}^{\infty}(x) dx. \quad (73)$$

The integral is solved numerically, and we find

$$\lim_{t \rightarrow \infty} \langle \tau^*(t) \rangle \langle \theta[-3 < x(t) < 3] \rangle = 8.91711 \dots \quad (74)$$

and $\langle \tau^*(t) \rangle$ is given in Eq. (26) with $\alpha = 3/4$. As mentioned, $\langle \theta[-3 < x(t) < 3] \rangle$ is the probability that a member of an ensemble of particles occupies the domain $[-3, 3]$ at time t . This prediction is tested in Fig. 10 showing that the non-normalized invariant density is the tool of choice to compute ensemble averages of integrable observables.

B. Time averages

The time integration over the pulse function observable (72) is the total time a trajectory $x(t')$ spends in the domain $[a, b]$ during the measurement time interval $(0, t)$; it will be denoted \bar{T} . For example, $[a, b]$ can be a domain in space including the resetting point or not. The total time the particle spends in $[a, b]$ is called the occupation time or the residence

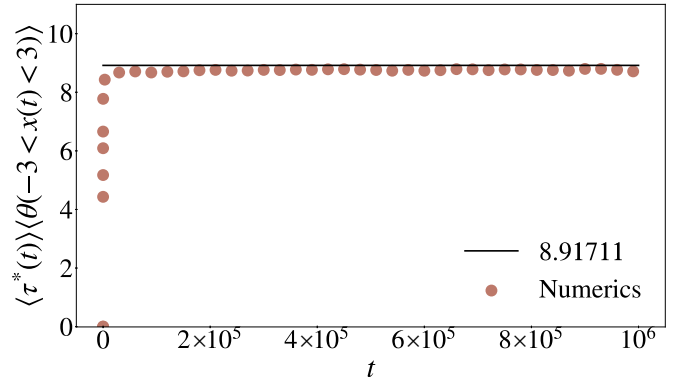


FIG. 10. Time evolution of $\langle \theta[-3 < x(t) < 3] \rangle$ times $\langle \tau^*(t) \rangle$ Eq. (26) for a Pareto PDF with $\alpha = 3/4$ and $t_0 = 1$. The solid line represents the long-time limit Eq. (74). Here $D = 1/2$, and we have used 10^6 trajectories.

time [48–50]. For thin-tailed distributions of resetting times, and using the ergodic hypothesis,

$$\lim_{t \rightarrow \infty} \frac{\int_0^t \theta(a < x(t') < b) dt'}{t} = \int_a^b \rho^{ss}(x) dx, \quad (75)$$

which is the probability a member of an ensemble of particles in NESS occupies the domain. We will treat this observable for the case $\alpha < 1$ below.

We now treat an integrable observable not restricting ourselves to an example. Then the ensemble-averaged time average

$$\langle \bar{\mathcal{O}}(t) \rangle \sim \frac{1}{t} \left\langle \int_0^t \mathcal{O}(t') dt' \right\rangle, \quad (76)$$

which is found by averaging many of the underlying processes, over time and over independent trajectories. Since the ensemble average in any experiment is simply a sum over a finite sample, we may replace the order of time and ensemble average, and then

$$\langle \bar{\mathcal{O}}(t) \rangle = \frac{\int_0^t \left[\int_{-\infty}^{\infty} \rho(x, t') \mathcal{O}(x) dx \right] dt'}{t}. \quad (77)$$

As before, in the long-time limit we replace the density $\rho(x, t)$ with the infinite density using Eq. (23), e.g. for $1/2 < \alpha < 1$,

$$\langle \bar{\mathcal{O}}(t) \rangle \sim \frac{\int_0^t \left[\int_{-\infty}^{\infty} \frac{\tilde{\mathcal{I}}^{\infty}(x)}{\langle \tau^*(t') \rangle} \mathcal{O}(x) dx \right] dt'}{t}. \quad (78)$$

In the numerator we can identify the ensemble average obtained with integration over the infinite density (69). Further, the time integration is straightforward, using Eqs. (69) and (70) we find

$$\lim_{t \rightarrow \infty} \frac{\langle \bar{\mathcal{O}}(t) \rangle}{\langle \mathcal{O}(t) \rangle} = \begin{cases} 1 & \text{for } \psi(\tau) \text{ thin-tailed} \\ \frac{1}{\alpha} & \frac{1}{2} < \alpha < 1 \\ 2 & 0 < \alpha < \frac{1}{2} \end{cases}. \quad (79)$$

We see that the time and ensemble averages are related to one another. For $\alpha < 1$ they are calculated using the infinite density otherwise by the normalized invariant density of the

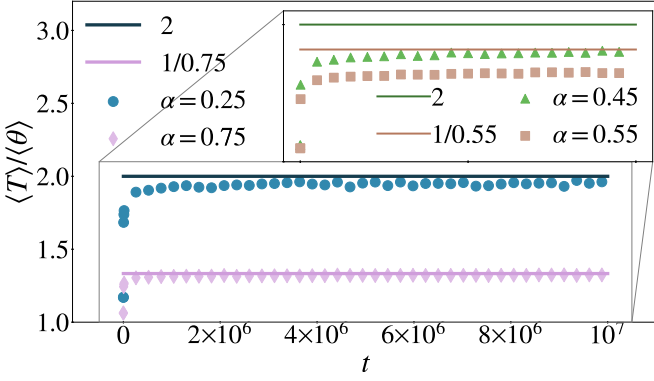


FIG. 11. Ratio between the ensemble-averaged time average and the ensemble average vs time. The observable is the pulse function (72) in the interval $-10 < x < 10$. We present numerical results for the Pareto reset time PDF with $t_0 = 1$ with $\alpha = 1/4$ and $\alpha = 3/4$. In solid lines the long-time limit of $\langle T \rangle / \langle \theta \rangle$, Eq. (79). In the inset figure, we present the same results but for α near the transition point below, $\alpha = 0.45$, and above, $\alpha = 0.55$. We can see that the agreement is not so good due to the slowing of the convergence near the transition in agreement with what is observed also in Fig. 12. Here $D = 1/2$ and we have used 10^7 trajectories.

NESS. The prefactors found for $\alpha < 1$ stem from simple time integration. We see that when $\alpha = 1$ and $\alpha = 1/2$ there is an ergodic transition in the system which, in principle, is easy to detect when α is tuned (the result in the first line holds for any distribution of resetting times, even a distribution that decays like a power law $\alpha > 1$, in such a way that the mean resetting time is finite). In Fig. 11 we show the comparison between the predictions in Eq. (79) with finite time simulations, showing excellent agreement without fitting.

Infinite ergodic theory deals also with the limiting laws of the distribution of time averages. We define a dimensionless variable

$$\eta = \frac{\bar{\mathcal{O}}}{\langle \mathcal{O} \rangle}, \quad (80)$$

where clearly the mean of η is unity. In what follows we assume that the observable is integrable, namely, the nonzero denominator is obtained in theory from the invariant density using Eqs. (69), (70), and (79) though a direct measurement in, e.g., an experiment or simulation is also a good possibility. For thin-tailed waiting time PDFs, η in the long-time limit is not fluctuating. In other words, its distribution is a δ function centered on unity.

C. Fluctuations of time averages

Consider the integral over the pulse function Eq. (72),

$$\eta = \frac{\int_0^t \theta(-a < x(t) < a) dt}{\langle \int_0^t \theta(-a < x(t) < a) dt \rangle} = \frac{\tilde{T}}{\langle \tilde{T} \rangle}. \quad (81)$$

Namely, we are interested in the statistics of the occupation time \tilde{T} in $[-a, a]$ when the observation is in $(0, t)$. Of course, the interval $[-a, a]$ contains the resetting point $x = 0$. In Eq. (81) η is normalized in the sense that its mean is unity.

The function $\theta[-a < x(t) < a]$ takes the value 1 when $x(t)$ is in the domain $[-a, a]$, 0 otherwise. By randomly switching between the values 1 and 0, the observable undergoes a dichotomous two-state process. What is the physical mechanism of the return into the domain $[-a, a]$? One possibility is that the resetting brings the particle back into the domain. For example, just before a resetting event, the particle might be positioned at $x(t) > a$, but after resetting, it is sent back to $-a < x = 0 < a$. Alternatively, the particle returns to the domain via the process of diffusion alone. We have here a competition between these two mechanisms of return. Recall that the PDF of resetting times is given by a fat-tailed law (6) while the PDF of first passage time of BM in an infinite domain in dimension one decays like $(\text{time})^{-3/2}$ [51], in the absence of resetting. Hence we might expect a transition in the ergodic properties of the system when $\alpha = 1/2$, which is also noticed in the behavior of the infinite invariant densities discussed above.

To quantify this behavior we use the EB parameter [52], defined as

$$\text{EB} = \frac{\langle \eta^2 \rangle - \langle \eta \rangle^2}{\langle \eta \rangle^2} = \frac{\langle \tilde{T}^2 \rangle - \langle \tilde{T} \rangle^2}{\langle \tilde{T} \rangle^2}. \quad (82)$$

An analysis of the EB parameter starts in the next section, and more details are found in Appendixes B and C. In the long-time limit

$$\text{EB} = \begin{cases} \alpha\pi - 1 + \frac{1}{2} \left[\frac{\pi\Gamma(1-\alpha)}{\Gamma(\frac{1}{2}-\alpha)} \right]^2, & 0 < \alpha < 1/2 \\ \frac{2\Gamma^2(1+\alpha)}{\Gamma(1+2\alpha)} - 1, & 1/2 < \alpha < 1 \\ 0, & \text{thin-tailed PDFs} \end{cases} \quad (83)$$

When the mean of the resetting time PDF is finite there is no ergodicity breaking as the PDF of η converges to a delta function and $\text{EB} = 0$. In contrast if $0 < \alpha < 1$ we have two types of behaviors. Note that when $\alpha \rightarrow 0$, we have $\text{EB} = (\pi/2) - 1 \simeq 0.57$. As shown below, just after Eq. (89) this is the value of the EB parameter for free BM (see also Appendix B).

When $1/2 < \alpha < 1$ the fluctuations we find are related to the fluctuations of the number of resets in the time interval $(0, t)$. More specifically recall that N is the random number of resets in the time interval $(0, t)$. The EB parameter for this observable is well known [52],

$$\text{EB} = \frac{\langle N^2 \rangle - \langle N \rangle^2}{\langle N \rangle^2} = \frac{2\Gamma^2(1+\alpha)}{\Gamma(1+2\alpha)} - 1, \quad (84)$$

which is valid for $0 < \alpha < 1$ and in the long-time limit. We see that the fluctuations of the time averages are related to the fluctuations of the number of resettings; however, this is true only when $1/2 < \alpha < 1$. The intuitive explanation is that when $1/2 < \alpha$ the return to the domain $[-a, a]$ is dominated by resetting and not by diffusion. Further, the time spent inside the domain $[-a, a]$ is statistically short compared to the time outside the domain, and so are the fluctuations of the latter that dominate the statistics of the time averages. The same is not true for thin-tailed PDFs where the mean times in and outside of the domain are both finite. Hence in the latter case we find ordinary ergodicity.

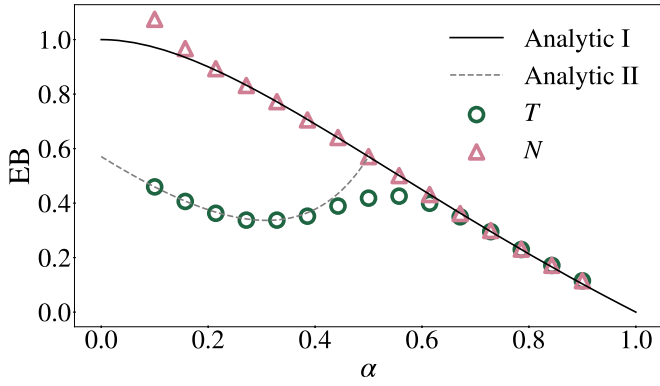


FIG. 12. EB parameter, describing the fluctuations of the time averages, vs α . Numerical results for the occupation time T for the reset process are presented, where we used $D = 1/2$, $a = 0.1$ the Pareto reset time PDF, with $t_0 = 1$. For $1/2 < \alpha < 1$, the EB parameter is the same as that for N (triangles), the number of resets up to time t . Close to the transition point $\alpha = 1/2$ we see deviations from theory, due to finite sampling and slowing of the convergence. When $0 < \alpha < 1/2$ the fluctuations are nontrivial, and we observe a minimum for the EB parameter. Here we have used 10^5 trajectories evolved to $t = 10^{10}$. We used Eq. (83) (Analytic II) and Eq. (84) (Analytic I) to present the theory.

To summarize, one can say that for $0 < \alpha < 1/2$ the fluctuations are less trivial if compared to other cases. As mentioned more technical details are provided below. In Fig. 12 we present numerical results for the EB parameter. We observe a minimum for the EB parameter found also in the context of a study of laser cooling [21]. The convergence of finite time simulations is poor close to the critical value of $\alpha = 1/2$, an effect that could be studied further.

IX. CALCULATING OCCUPATION TIME STATISTICS WITH CTRW FORMALISM

The study of time averages is related to the theory of functionals of stochastic processes as the observable, which is a function of the random path, is integrated over time. The theory of Brownian functionals with resetting was studied in [53,54]. Here one of our main goals is to show how tools from continuous time random walk (CTRW) theory can be applied for this aim.

As mentioned, we call the time spent by the resetting process $x(t)$ in the spatial domain $[-a, a]$, within the time window $(0, t)$, \tilde{T} , where the resetting is to the origin $x = 0$. The PDF of this random variable will be denoted $P(\tilde{T}, t)$. For standard ergodic processes, and in the limit of long times, we expect that this PDF becomes a narrow distribution, centered around the mean, as mentioned already. However, when $\alpha < 1$ this is not true anymore. To analyze this issue, we use a tool developed by Montroll, Weiss, and others in the context of CTRWs [39]. The same tool was used to study the ergodic properties of subrecoil laser-cooled gases [21]. Here the first goal is to relate between statistics of occupation times of Brownian motion and those of the occupation times of the reset process. Second, we derive the basic formulas of infinite ergodic theory from a well-known approach and further

provide simple intuitive formulas for averages. We start with a recap of occupation time statistics for Brownian motion.

A. Occupation time for Brownian motion

Consider reset free Brownian motion $x_{\text{BM}}(t)$ starting at the origin $x = 0$. The occupation time of the process is

$$T_{\text{BM}}(t) = \int_0^t \theta[x_{\text{BM}}(t')] dt'. \quad (85)$$

Here and in what follows we use $\theta[x_{\text{BM}}(t)] = \theta[-a < x_{\text{BM}}(t) < a]$ as a short-hand notation. The mean of the pulse function is obtained from the Gaussian packet

$$\langle \theta[x_{\text{BM}}(t)] \rangle = \int_{-\infty}^{\infty} G(x, t) \theta[x] dx. \quad (86)$$

Hence the mean occupation time is $\langle T(t) \rangle_{\text{BM}} = \int_0^t \langle \theta[x_{\text{BM}}(t')] \rangle dt'$, and using Eq. (1) it is easy to show that

$$\begin{aligned} \langle T(t) \rangle_{\text{BM}} = & t + \frac{a\sqrt{t}}{\sqrt{\pi D}} \exp\left(-\frac{a^2}{4Dt}\right) \\ & - \left(t + \frac{a^2}{2D}\right) \text{Erfc}\left(\frac{a}{\sqrt{4Dt}}\right). \end{aligned} \quad (87)$$

In the long-time limit

$$\langle T(t) \rangle_{\text{BM}} \sim \frac{2a}{\sqrt{\pi D}} t^{1/2}. \quad (88)$$

The distribution of the occupation time of Brownian motion is discussed further in Appendix B. Using the Feynman-Kac formalism [55,56], the PDF of the occupation time in the long-time limit is half a Gaussian

$$\text{PDF}_{\text{BM}}(T|t) \sim \left(\frac{D}{\pi a^2 t}\right)^{1/2} \exp\left(-\frac{DT^2}{4a^2 t}\right). \quad (89)$$

The Laplace transform of the finite time solution is presented in Appendix B. The long-time limit of the EB parameter is $\text{EB} = (\langle T^2 \rangle_{\text{BM}} - \langle T \rangle_{\text{BM}}^2) / \langle T \rangle_{\text{BM}}^2 = (\pi/2) - 1$, namely, the same as the reset process (83) when $\alpha \rightarrow 0$.

B. Occupation time for the resetting problem

The occupation time of the reset process $\tilde{T}(t) = \int_0^t \theta[x(t')] dt'$ is now considered. With the notation for time averages (66) and for the pulse function observable $\bar{O} = \tilde{T}/t$. Let $Q_N(\tilde{T}, t) dt d\tilde{T}$ be the probability that the N th resetting event takes place in the time interval $(t, t + dt)$ when the value of the occupation time is within $(\tilde{T}, \tilde{T} + d\tilde{T})$. This function is given by the iteration rule

$$Q_{N+1}(\tilde{T}, t) = \int_0^{\tilde{T}} dT' \int_0^t d\tau Q_N(\tilde{T} - T', t - \tau) \phi(T', \tau). \quad (90)$$

Here $\phi(T', \tau)$ is the joint PDF of the resetting interval τ , i.e., the time between consecutive resets, and the occupation time in the same interval T' . According to Eq. (3) the resetting process is defined with a sequence of time intervals between resettings

$$\{\tau_1, \tau_2, \dots, \tau_N, B\}.$$

Within each resetting interval τ_i we have an occupation time T_i in the spatial domain $(-a, a)$. Given the reset time interval τ_i , statistical properties of T_i are determined by the laws of Brownian motion. Clearly, the occupation time for the reset process is

$$\tilde{T} = \sum_{i=1}^N T_i + T_B. \quad (91)$$

T_B is the occupation time in the interval $(-a, a)$ gained in the backward time B . The sets $\{T_i\}$ and $\{\tau_i\}$ are separately composed from IID random variables; however, T_i and τ_i are mutually dependent. The longer is τ_i the longer T_i is, in a statistical sense. The joint PDF of the pair is

$$\phi(T, \tau) = \psi(\tau) \text{PDF}_{\text{BM}}(T|\tau), \quad (92)$$

where here we use the PDF of occupation times for Brownian motion without restarts.

Equation (90) describes the basic property of the process. To arrive in \tilde{T} at time t when the previous resetting took place at $t - \tau$, the previous value of \tilde{T} , at the moment of the previous resetting, was $\tilde{T} - T$. Notice that in Eq. (90) time t denotes a dot on the time axis, on which a resetting took place (see details below). Solving Eq. (90) is possible with the help of the convolution theorem of a Laplace transform. Let

$$\hat{Q}_N(p, s) = \int_0^\infty d\tilde{T} \int_0^\infty dt \exp(-p\tilde{T} - st) Q_N(\tilde{T}, t) \quad (93)$$

be the double Laplace transform of $Q_N(\tilde{T}, t)$ where $p \leftrightarrow \tilde{T}$ and $s \leftrightarrow t$ are Laplace pairs. The convolution theorem and the iteration rule give $\hat{Q}_{N+1}(p, s) = \hat{Q}_N(p, s) \hat{\phi}(p, s)$ where $\hat{\phi}(p, s)$ is the double Laplace transform of $\phi(T, \tau)$. Using the seed, $Q_0(\tilde{T}, t) = \delta(\tilde{T})\delta(t)$, reflecting the initial condition, namely, that the resetting process starts at time $t = 0$, we have

$$\hat{Q}_N(p, s) = [\hat{\phi}(p, s)]^N. \quad (94)$$

The PDF $P(\tilde{T}, t)$ is in turn given by

$$P(\tilde{T}, t) = \sum_{N=0}^{\infty} \int_0^{\tilde{T}} dT'_B \int_0^t dB Q_N(\tilde{T} - T'_B, t - B) \Phi(T_B, B). \quad (95)$$

Here we summed over the number of restarts N and considered the fact that the observation time t is found at a time B after the last resetting event in the sequence. We further integrate over the backward recurrence time. Finally, the statistical weight function is

$$\Phi(T_B, B) = S(B) \text{PDF}_{\text{BM}}(T_B|B), \quad (96)$$

where, like before, $S(B) = \int_B^\infty \psi(\tau) d\tau$ is the survival probability, i.e., the probability of not resetting. We will soon use the Laplace $B \rightarrow s$ transform of this function $\hat{S}(s) = [1 - \hat{\psi}(s)]/s$ where $\hat{\psi}(s)$ is the Laplace transform of $\psi(\tau)$.

Now we again use the convolution theorem. Let $\hat{P}(p, s)$ be the double Laplace transform of $P(\tilde{T}, t)$. Using Eq. (95),

$$\hat{P}(p, s) = \sum_{N=0}^{\infty} \hat{Q}_N(p, s) \hat{\phi}(p, s), \quad (97)$$

where

$$\hat{\phi}(p, s) = \int_0^\infty \int_0^\infty \exp[-T_B p - Bs] \times S(B) \text{PDF}_{\text{BM}}(T_B|B) dT_B dB. \quad (98)$$

Inserting Eqs. (94) and (97) and summing the geometric series,

$$\hat{P}(p, s) = \frac{\hat{\phi}(p, s)}{1 - \hat{\phi}(p, s)}. \quad (99)$$

In the context of CTRW such an equation is used to analyze the positional PDF of the packet of particles, though then usually one invokes a Fourier-Laplace transform [39,57–59]. The inversion of the formal solution Eq. (99) to the (\tilde{T}, t) domain is a significant problem, which can be tackled analytically in the long-time limit. In particular, from the definition of the Laplace transform

$$\begin{aligned} \hat{P}(p, s) &= \int_0^\infty d\tilde{T} \int_0^\infty dt \exp[-p\tilde{T} - st] P(\tilde{T}, t) \\ &= \int_0^\infty (1 - p\tilde{T} + \dots) d\tilde{T} \int_0^\infty dt e^{-st} P(\tilde{T}, t) \\ &= \frac{1}{s} - p \langle \tilde{T}(s) \rangle \dots, \end{aligned}$$

where we used the normalization condition for $P(\tilde{T}, t)$ and $\langle \hat{\tilde{T}}(s) \rangle$ is the Laplace $t \rightarrow s$ transform of the mean occupation time $\langle \tilde{T}(t) \rangle$. Another way to write this is

$$\langle \hat{\tilde{T}}(s) \rangle = - \frac{\partial \hat{P}(p, s)}{\partial p} \Big|_{p=0}. \quad (100)$$

Using the Montroll-Weiss-like equation (99) we find

$$\langle \hat{\tilde{T}}(s) \rangle = - \frac{\partial_p \hat{\phi}(p, s)|_{p=0}}{1 - \hat{\phi}(p=0, s)} - \frac{\partial_p \phi(p, s)|_{p=0} \hat{\phi}(p=0, s)}{[1 - \phi(p=0, s)]^2}. \quad (101)$$

A similar approach can be used to find the variance of the occupation time; however, here will study only the mean.

We use $\hat{\phi}(p=0, s) = \hat{\psi}(s)$, $\hat{\Phi}(p=0, s) = [1 - \hat{\psi}(s)]/s$, and

$$\partial_p \hat{\phi}(p, s)|_{p=0} = - \int_0^\infty \exp(-s\tau) \langle T(\tau) \rangle_{\text{BM}} \psi(\tau) d\tau, \quad (102)$$

where

$$\langle T(\tau) \rangle_{\text{BM}} = \int_0^\infty T \text{PDF}_{\text{BM}}(T|\tau) dT \quad (103)$$

is the mean occupation time of a Brownian motion in $(-a, a)$, in the time interval $(0, \tau)$. Similarly

$$\partial_p \hat{\Phi}(p, s)|_{p=0} = - \int_0^\infty \exp(-sB) \langle T(B) \rangle_{\text{BM}} S(B) dB. \quad (104)$$

Using Eqs. (101), (102), and (104) we find

$$\langle \hat{T}(s) \rangle = \underbrace{\frac{\int_0^\infty \langle T(\tau) \rangle_{\text{BM}} \psi(\tau) e^{-s\tau} d\tau}{s[1 - \hat{\psi}(s)]}}_{\mathcal{T}_1(s)} + \underbrace{\frac{\int_0^\infty \langle T(B) \rangle_{\text{BM}} S(B) e^{-sB} dB}{1 - \hat{\psi}(s)}}_{\mathcal{T}_2(s)}. \quad (105)$$

This formula relates the mean occupation time of the resetting process, the mean occupation time of the restart-free Brownian motion, and the waiting time $\psi(\tau)$. We note that Eq. (105) can be generalized to other observables beyond the occupation time. The two contributions defined in this equation, $\mathcal{T}_1(s)$ and $\mathcal{T}_2(s)$, describe contributions to the occupation time before and after the last reset event in the sequence.

1. Mean occupation time $1/2 < \alpha < 1$

To analyze the long-time behavior of the mean occupation time we consider the small s limit, following a standard approach by considering Eq. (45), which holds for $0 < \alpha < 1$. We now need to distinguish between three cases. A short calculation, valid when $1/2 < \alpha < 1$, will convince the reader that the leading term, when $s \rightarrow 0$ in Eq. (105) reads

$$\langle \hat{T}(s) \rangle \sim \frac{\int_0^\infty \langle T(\tau) \rangle_{\text{BM}} \psi(\tau) d\tau}{b_\alpha s^{1+\alpha}}, \quad (106)$$

and only $\mathcal{T}_1(s)$ is contributing to this limit. Inverting to the time domain we find in the long-time limit

$$\langle \tilde{T}(t) \rangle \sim \frac{t^\alpha}{\Gamma(1 + \alpha) b_\alpha} \int_0^\infty \langle T(\tau) \rangle_{\text{BM}} \psi(\tau) d\tau. \quad (107)$$

Noticing that the average number of restarts is $\langle N(t) \rangle_{\text{Res}} \sim t^\alpha / b_\alpha \Gamma(1 + \alpha)$ we have

$$\langle \tilde{T}(t) \rangle \sim \langle N(t) \rangle_{\text{Res}} \langle \langle T \rangle_{\text{BM}} \rangle_{\text{Res}}, \quad (108)$$

where the mean of the occupation time, within a resetting period, averaged over the resetting time is

$$\langle \langle T \rangle_{\text{BM}} \rangle_{\text{Res}} = \int_0^\infty \int_0^\infty T \text{PDF}_{\text{BM}}(T|\tau) dT \psi(\tau) d\tau. \quad (109)$$

In Eqs. (108) and (109) we distinguish between averages over the resetting time and averages over the Brownian motion within each interval. Equation (108) is expected; a main point to notice is that it is not valid when $0 < \alpha < 1/2$. Since $\langle T(\tau) \rangle_{\text{BM}} \sim \tau^{1/2}$, when averaging over $\psi(\tau) \propto \tau^{-1-\alpha}$, the integral in Eq. (109) diverges when $\alpha < 1/2$, a case soon to be treated.

Equation (108) remains valid for the case where the mean of the waiting time between resets is finite, for example, when $\psi(\tau)$ is an exponential function. The difference is that $\langle N(t) \rangle_{\text{Res}} \sim t/\langle \tau \rangle$, where $\langle \tau \rangle$ is the mean time between restarts.

How is Eq. (106) related to the non-normalized invariant density when $1/2 < \alpha < 1$? We use the pulse function (72) of

a Brownian path without resetting

$$\begin{aligned} \langle T(\tau) \rangle_{\text{BM}} &= \left\langle \int_0^\tau \theta[x(t')] dt' \right\rangle_{\text{BM}} = \int_0^\tau \langle \theta[x(t')] \rangle dt' \\ &= \int_0^\tau \int_{-\infty}^\infty \theta[x] G(x, t') dx dt' \end{aligned} \quad (110)$$

as mentioned already. Using Eq. (108) the occupation time for the resetting process is

$$\langle \tilde{T}(t) \rangle \sim \langle N(t) \rangle_{\text{Res}} \int_0^\infty d\tau \int_{-\infty}^\infty dx G(x, \tau) \theta(x) [-\partial_\tau S(\tau)], \quad (111)$$

where we apply $\psi(\tau) = -\partial_\tau S(\tau)$. Integrating by parts, and employing Eq. (23),

$$\langle \tilde{T}(t) \rangle \sim \langle N(t) \rangle_{\text{Res}} \int_{-\infty}^\infty \theta(x) \mathcal{I}^\infty(x) dx, \quad (112)$$

which for the observable of interest, namely, the pulse function reads $\langle \tilde{T}(t) \rangle \sim \langle N(t) \rangle_{\text{Res}} \int_{-a}^a \mathcal{I}^\infty(x) dx$. By definition $\langle \tilde{T}(t) \rangle / t = \langle \bar{\theta}[x(t)] \rangle$ and hence the CTRW approach and Eq. (112) yield the same result as in Eq. (79) utilizing Eqs. (14) and (69) and the long-time identity $\partial_t \langle N(t) \rangle_{\text{Res}} / \alpha = \langle N(t) \rangle_{\text{Res}} / t$.

2. Mean occupation time $0 < \alpha < 1/2$

We now analyze the case $0 < \alpha < 1/2$. Here contributions to the mean occupation time stem from both terms in Eq. (105), namely, now the backward recurrence time is large in a statistical sense, in a way that it contributes to the averaged observable also in the long-time limit. In the small s limit, we use the asymptotic formula (88) and find employing Eq. (105) and $1 - \hat{\psi}(s) \sim b_\alpha s^\alpha$

$$\mathcal{T}_1(s) \sim \frac{2a}{\sqrt{\pi D}} \frac{\int_0^\infty \tau^{1/2} (\tau_0)^\alpha \tau^{-1-\alpha} \exp(-s\tau) d\tau}{b_\alpha s^{1+\alpha}}, \quad (113)$$

where we used Eq. (6). Inserting the definition of b_α given in Eq. (45) and integrating we find for small s

$$\mathcal{T}_1(s) \sim \frac{2\alpha a}{\Gamma(1 - \alpha) \sqrt{\pi D}} \Gamma(1/2 - \alpha) s^{-3/2}. \quad (114)$$

Inverting to the time domain we find

$$\mathcal{T}_1(t) \sim \frac{4a}{\pi \sqrt{D}} \frac{\Gamma(1/2 - \alpha)}{|\Gamma(-\alpha)|} t^{1/2}. \quad (115)$$

The second contribution is analyzed similarly, in particular employing Eq. (88),

$$\mathcal{T}_2(s) \sim \frac{2a}{\sqrt{\pi D}} \frac{\int_0^\infty \sqrt{B} S(B) \exp(-sB) dB}{b_\alpha s^\alpha}. \quad (116)$$

Using $S(B) \sim (\tau_0)^\alpha \tau^{-\alpha} / \alpha$ obtained from Eq. (6), integrating, and then inverting to the time domain we find

$$\mathcal{T}_2(t) \sim \frac{4a}{\pi \sqrt{D}} \frac{\Gamma(3/2 - \alpha)}{\Gamma(1 - \alpha)} t^{1/2}. \quad (117)$$

Summing Eqs. (115) and (117) we get the mean occupation time

$$\langle \tilde{T}(t) \rangle \sim \frac{2a}{\pi \sqrt{D}} \frac{\Gamma(1/2 - \alpha)}{\Gamma(1 - \alpha)} t^{1/2}. \quad (118)$$

When $\alpha \rightarrow 0$ we obtain the same result as found for Brownian motion, Eq. (88), while in the limit $\alpha \rightarrow 1/2$ this expression diverges signaling the transition.

The same result can be obtained from the infinite density approach. Since the occupation time is the time integral of the pulse function

$$\frac{\langle \tilde{T}(t) \rangle}{t} \sim 2\langle \theta(x) \rangle, \quad (119)$$

where we used Eq. (79), which gives the prefactor 2. The average $\langle \theta(x) \rangle$ is with respect to the infinite invariant density as in Eq. (70):

$$\langle \theta(x) \rangle \sim \frac{\int_{-\infty}^{\infty} \theta(x) \mathcal{I}^{\infty}(x) dx}{\sqrt{2Dt}}. \quad (120)$$

As mentioned in Eq. (24) the infinite density is a constant in this case. It is then easy to show that the results obtained with the CTRW approach are the same as those found with the infinite density method. Of course, this is what is expected, though here once we have the infinite density, the calculation is straightforward, as is the case of ergodic processes, where time integration is replaced with a phase space integration. In Appendix B we continue with this line of study and calculate the fluctuations of the time averages, which are needed to obtain the EB parameter.

X. DISCUSSION

Relating the NESS to the limiting laws of the backward recurrence times [12–14] was our starting point. This is a valuable tool for many restart models, where the reset erases the memory of the process, and is not limited to BM. As studied in [41] the erasure of memory, which is clearly valid for a Markovian BM, is not the general rule. Using statistics of the backward recurrence time we simplified main expressions for NESS (that previously relied on Laplace transforms) and obtained results which were found previously with other methods [4,6,15]. We also added ingredients to the resetting literature.

The tools of infinite ergodic theory and the non-normalized NESS are employed to obtain general ergodic aspects of the restart process. The invariant densities can be normalized or non-normalized, but their functional dependence on the survival probability appears similar. Thus, by controlling the distribution of resetting time we can explore either the standard ergodic phase or the theory of infinite ergodic theory. The timescale $\langle \tau^*(t) \rangle$ and the length scale $\sqrt{2Dt}$ are used to relate the infinite density $\tilde{T}^{\infty}(x)$ with the probability density $\rho(x, t)$, for $1/2 < \alpha < 1$ and $0 < \alpha < 1/2$, respectively [see Eqs. (23) and (24)].

The behaviors of both time and ensemble averages were addressed. When dealing with thin-tailed distributions the standard ergodic picture emerges. The exception is sharp restart, which has no NESS. The case of sporadic resetting with fat-tailed distributed resetting times was the main focus of this study. A statistical theory of the time averages works as follows. When $\alpha < 1$ we first check that the observable is integrable with respect to the non-normalized state. In this case we find the ensemble average using the infinite invariant

density. Once this is known, we use Eq. (79) to obtain the ensemble average of the time average $\langle \bar{O} \rangle$. We then studied the fluctuations of the time averages, focusing on an integrable observable, namely, the pulse function. The time integral of this observable is the total time spent in an interval, called the occupation time. The fluctuations exhibited nontrivial effects, and a transition in the EB parameter was found for $\alpha = 1/2$. Additionally, $\alpha = 1/2$ marks a transition in the structure of the infinite invariant density itself. We further pointed out that when $1/2 < \alpha < 1$ the EB parameter of the time average is the same as the one computed for the fluctuations of the number of renewals. This implies that the fluctuations in this phase are universal, and independent of the observable, as long as it is integrable; however, we did not prove this statement. In contrast, when $0 < \alpha < 1/2$ the fluctuations of time averages, and the EB parameter, depend on the observable and hence nonuniversal.

We speculate that this type of transition is generic and can be found similarly in other processes. As we showed, in our case the transition is found when α matches the exponent describing the PDF of first passage times of a Brownian motion on a line in the absence of resetting. The latter well-known PDF, with absorption at, e.g., $x = 0$, decays like (first passage time) $^{-(1+\beta)}$ and $\beta = 1/2$ in dimension one. In many other processes $\beta \neq 1/2$, for example, for diffusion in a potential that grows like the log of the distance, subdiffusive CTRW, random walks on some fractals or comb structures, etc. We believe that when $\alpha = \beta < 1$ the resetting process might exhibit a transition similar to what we found here, but the details and the generality of this statement must be worked out. Finally, we have studied the uniform approximation, for both B and for the coordinate x of the reset particle. This approach gives the probability density $\rho(x, t)$ for small and large x and was shown to yield statistical quantities also for intermediate timescales. It tackles the problem of slowing down when $\alpha = 1/2$. From this excellent approximation, we find the fractional equation (57), which is a simple tool for the calculation of $\rho(x, t)$.

XI. CONCLUSIONS

We showed how the analysis of the statistics of the backward recurrence time solves the NESS of the restart process. Two types of invariant densities are present in this problem. These are the normalized and non-normalized invariant densities, for thin-tailed or fat-tailed resetting time PDFs, respectively. We uncovered two ergodic transitions. The first takes place when the mean waiting time diverges. The second is found when $\alpha = 1/2$. At this critical value of α the infinite density changes its structure. Further, the EB parameter exhibits a nonanalytical behavior. Thus both time and ensemble averages have vastly different behaviors when $\alpha < 1/2$ compared to $1/2 < \alpha < 1$. Physically this ergodic transition is found due to the competition between return mechanisms to the origin. We also found slow convergence to asymptotic limits. To tackle this issue we used the uniform approximation. We use a simple fractional integral equation to this end, connecting fractional calculus to the calculation of the density of particles.

ACKNOWLEDGMENTS

The support of the Israel Science Foundation (E.B.) and the Spanish government (R.F., V.M.) under Grants No. 1614/21 and No. PID2021-122893NB-C22, respectively, is acknowledged. The authors also acknowledge the helpful comments and discussions with Dr. Axel Masó-Puigdellosas.

APPENDIX A

If $\langle \tau \rangle$ is finite, our results for the NESS reduce to those found previously by Pal, Kundu, and Evans (PKE) [4]. PKE consider BM under a time-modulated resetting protocol. The rate of resetting is $r(t)$, and it is a function of time t since the last reset event. We fix the resetting position at $x = 0$. To see that this model is the same as the one considered here, we identify $S(\tau) = \exp[-R(\tau)]$ where $R(\tau) = \int_0^\tau r(t') dt'$; hence the PDF of times between resetting is

$$\psi(\tau) = -\frac{d}{d\tau} S(\tau) = r(\tau) \exp[-R(\tau)]. \quad (\text{A1})$$

PKE find the NESS using Laplace transforms

$$\rho^{\text{ss}}(x) = \lim_{s \rightarrow 0} \frac{\hat{Q}(x, s)}{\hat{\mathcal{H}}_r(s)}. \quad (\text{A2})$$

In the numerator $\hat{Q}(x, s) = \int_0^\infty dt \exp[-st - R(t)] G(x, t)$ and $G(x, t)$ is the Gaussian Green function of the BM (1). Since as mentioned $\exp[-R(t)]$ is the survival probability, $S(t)$ in our notation, and taking the $s \rightarrow 0$ limit, we get

$$\lim_{s \rightarrow 0} \hat{Q}(x, s) = \int_0^\infty S(\tau) G(x, \tau) d\tau. \quad (\text{A3})$$

This is the same as the function on the right-hand side of Eq. (17). Further using PKE's results,

$$\lim_{s \rightarrow 0} \hat{\mathcal{H}}_r(s) = \int_0^\infty d\tau e^{-R(\tau)}$$

$$= \int_0^\infty d\tau S(\tau) = - \int_0^\infty d\tau \tau \frac{dS(\tau)}{d\tau} = \langle \tau \rangle. \quad (\text{A4})$$

Hence we see that PKEs result (A2) is the same as Eq. (17).

APPENDIX B

Consider one-dimensional Brownian motion starting at x_0 . The PDF of the occupation time, in the spatial domain $(-a, a)$, is denoted $\text{PDF}_{\text{BM}}(T|t)$. Clearly, this PDF is a function of x_0 though, in the main text, we study $x_0 = 0$. Let $g_{x_0}(p; t)$ be the Laplace transform

$$g_{x_0}(p; t) = \int_0^\infty \exp(-pT) \text{PDF}_{\text{BM}}(T|t) dT. \quad (\text{B1})$$

The backward Feynman-Kac equation reads [56,61]

$$\partial_t g_{x_0}(p; t) = D \frac{\partial^2 g_{x_0}(p; t)}{\partial (x_0)^2} - p\theta[x_0] g_{x_0}(p; t). \quad (\text{B2})$$

As is well known this is the Schrödinger equation for imaginary time. In this analogy $p\theta[x]$ acts like a potential of force, a square barrier in our case. Initially $g_{x_0}(T, t) = \delta(T)$ since the occupation time is zero at the initial time, and hence employing the Laplace transform we get $g_{x_0}(p; t)|_{t=0} = 1$. We now consider a second Laplace transform

$$g_{x_0}(p; s) = \int_0^\infty \exp(-st) g_{x_0}(p; t) dt. \quad (\text{B3})$$

The variables in the parentheses of the function define the space we are working in. Using Eq. (B2) and the initial condition

$$s g_{x_0}(p; s) - 1 = D \frac{\partial^2 g_{x_0}(p; s)}{\partial (x_0)^2} - p\theta[x_0] g_{x_0}(p; s). \quad (\text{B4})$$

Using the pulse function, $\theta(x_0) = 1$ in $-a < x_0 < a$ otherwise zero, we have three regions:

$$g_{x_0}(p; s) = \begin{cases} c_0 \exp\left(\frac{x_0 \sqrt{s}}{\sqrt{D}}\right) + \frac{1}{s} & x_0 < -a \\ c_1 \exp\left(\frac{x_0 \sqrt{s+p}}{\sqrt{D}}\right) + c_2 \exp\left(-\frac{x_0 \sqrt{s+p}}{\sqrt{D}}\right) + \frac{1}{s+p} & -a < x_0 < a. \\ c_3 \exp\left(-\frac{x_0 \sqrt{s}}{\sqrt{D}}\right) + \frac{1}{s} & x_0 > a \end{cases} \quad (\text{B5})$$

Here c_0, c_1, c_2, c_3 are constants independent of x_0 . Since $g_{x_0}(p; s) = g_{-x_0}(p; s)$ from symmetry, $c_1 = c_2$ and $c_0 = c_3$. We use the boundary at $x_0 = -a$ and from the continuity condition

$$c_0 \exp\left(-\frac{a \sqrt{s}}{\sqrt{D}}\right) + \frac{1}{s} = c_1 \left[\exp\left(-\frac{a \sqrt{s+p}}{\sqrt{D}}\right) + \exp\left(\frac{a \sqrt{s+p}}{\sqrt{D}}\right) \right] + \frac{1}{s+p}. \quad (\text{B6})$$

Further from the continuity of the fluxes at the boundary namely, $\partial_{x_0} g_{x_0}(p; s)|_{x_0=-a-\epsilon} = \partial_{x_0} g_{x_0}(p; s)|_{x_0=-a+\epsilon}$ when $\epsilon \rightarrow 0$, we get

$$c_0 \sqrt{s} \exp\left(-\frac{a \sqrt{s}}{\sqrt{D}}\right) = -2c_1 \sqrt{s+p} \sinh\left(\frac{a \sqrt{s+p}}{\sqrt{D}}\right). \quad (\text{B7})$$

Solving and setting $x_0 = 0$, which greatly simplifies the solution, we find

$$g_0(p; s) = \frac{p}{s(s+p) \left[\cosh\left(\frac{a \sqrt{s+p}}{\sqrt{D}}\right) + \sqrt{1 + \frac{p}{s}} \sinh\left(\frac{a \sqrt{s+p}}{\sqrt{D}}\right) \right]} + \frac{1}{s+p}. \quad (\text{B8})$$

Setting $p = 0$ we have $g_0(0, s) = 1/s$ which is the normalization condition. As usual, we have the expansion

$$g_0(p; s) \sim \frac{1}{s} - p \langle \hat{T}(s) \rangle_{\text{BM}} + \frac{p^2 \langle \hat{T}^2(s) \rangle_{\text{BM}}}{2} \dots \quad (\text{B9})$$

Hence the small p expansion of Eq. (B8) yields the moments of the occupation time for $x_0 = 0$. For example,

$$\langle T(s) \rangle_{\text{BM}} = \frac{1 - \exp\left(\frac{-a\sqrt{s}}{\sqrt{D}}\right)}{s^2}. \quad (\text{B10})$$

The inverse Laplace transform gives Eq. (87). The second moment $\langle T^2(s) \rangle_{\text{BM}}$ is similarly found using a program like *Mathematica*, though the expression is already cumbersome. Focusing on the long-time limit, we consider the small s expansion and find $\langle \hat{T}^2(s) \rangle_{\text{BM}} \sim 2a^2/(Ds^2)$ inverting yields $\langle T^2(t) \rangle_{\text{BM}} \sim 2a^2 t/D$, which in turn gives $\text{EB} = (\pi/2) - 1$ as mentioned in the text. Finally, to find the long-time limit, we expand the solution for small s and p finding

$$g_0(p; s) \sim \frac{\sqrt{D/a^2 s^{-1/2}}}{p + \sqrt{D/a^2 s^{1/2}}}. \quad (\text{B11})$$

Inverting from $p \rightarrow T$ and then $s \rightarrow t$ we find the half Gaussian PDF of the occupation time Eq. (89).

APPENDIX C

1. Mean square occupation time

From the PDF of the occupation time in the Laplace space, the mean square occupation time may be found from

$$\langle \tilde{T}^2(s) \rangle = \left[\frac{\partial^2 \hat{P}(p, s)}{\partial p^2} \right]_{p=0}. \quad (\text{C1})$$

Using Eq. (99) we find

$$\frac{\partial^2 \hat{P}(p, s)}{\partial p^2} = \frac{\partial_{pp} \hat{\Phi}}{1 - \hat{\Phi}} + 2 \frac{\partial_p \hat{\Phi} \partial_p \hat{\Phi}}{(1 - \hat{\Phi})^2} + \frac{\hat{\Phi} \partial_{pp} \hat{\Phi}}{(1 - \hat{\Phi})^2} + 2 \frac{\hat{\Phi} (\partial_p \hat{\Phi})^2}{(1 - \hat{\Phi})^3} \quad (\text{C2})$$

and from Eqs. (92) and (98) we get

$$\partial_{pp} \hat{\Phi}|_{p=0} = \int_0^\infty e^{-s\tau} \psi(\tau) \langle T^2(\tau) \rangle_{\text{BM}} \equiv I_2(s) \quad (\text{C3})$$

and

$$\partial_{pp} \hat{\Phi}|_{p=0} = \int_0^\infty e^{-sB} S(B) \langle T^2(B) \rangle_{\text{BM}} \equiv I_2^*(s). \quad (\text{C4})$$

Defining $\partial_p \hat{\Phi}|_{p=0} = -I_1(s)$ and $\partial_p \hat{\Phi}|_{p=0} = -I_1^*(s)$ and from (C1) and (C2) we have

$$\begin{aligned} \langle \tilde{T}^2(s) \rangle &= \frac{I_2^*(s)}{1 - \hat{\psi}(s)} + \frac{2I_1(s)I_1^*(s)}{(1 - \hat{\psi}(s))^2} \\ &+ \frac{I_2(s)}{s(1 - \hat{\psi}(s))} + \frac{2I_1(s)^2}{s(1 - \hat{\psi}(s))^2} \end{aligned} \quad (\text{C5})$$

and the mean occupation time given in Eq. (100) can be rewritten as

$$\langle \tilde{T}(s) \rangle = \frac{I_1^*(s)}{1 - \hat{\psi}(s)} + \frac{I_1(s)}{s(1 - \hat{\psi}(s))}. \quad (\text{C6})$$

2. Exponential resetting

Let us obtain first the mean occupation time and the mean square occupation time for exponential resetting. Considering $\psi(\tau) = re^{-r\tau}$ we find $I_1(s) = r \langle \hat{T}(s+r) \rangle_{\text{BM}}$, $I_1^*(s) = \langle \hat{T}(s+r) \rangle_{\text{BM}}$, $I_2(s) = r \langle \hat{T}^2(s+r) \rangle_{\text{BM}}$, $I_2^*(s) = \langle \hat{T}^2(s+r) \rangle_{\text{BM}}$. In consequence, (C6) has the form

$$\langle \tilde{T}(s) \rangle = \left(\frac{r+s}{s} \right)^2 \langle \hat{T}(s+r) \rangle_{\text{BM}}.$$

In the long-time limit $s \rightarrow 0$

$$\langle \tilde{T}(s) \rangle \simeq \frac{r^2}{s^2} \langle \hat{T}(r) \rangle_{\text{BM}}$$

so that in the real time

$$\langle T(t) \rangle \simeq \langle \hat{T}(r) \rangle_{\text{BM}} r^2 t = t(1 - e^{-a\sqrt{r/D}}).$$

Analogously,

$$\begin{aligned} \langle \tilde{T}^2(s) \rangle &= \left(1 + \frac{r}{s} \right)^2 \left[\langle \hat{T}^2(s+r) \rangle_{\text{BM}} \right. \\ &\quad \left. + 2r \left(1 + \frac{r}{s} \right) \langle (\hat{T}(s+r))_{\text{BM}}^2 \rangle \right], \end{aligned}$$

which in the limit $s \rightarrow 0$

$$\langle \tilde{T}^2(s) \rangle \simeq 2 \frac{r^4}{s^3} \langle (\hat{T}(r))_{\text{BM}}^2 \rangle$$

so that in the real time

$$\langle T^2(t) \rangle \simeq t^2 (1 - e^{-a\sqrt{r/D}})^2.$$

We see that $\langle T^2(t) \rangle = \langle T(t) \rangle^2$ so that $\text{EB} = 0$.

3. Long-tailed resetting

a. Mean occupation time

Now we consider the long-tailed resetting PDFs using

$$\psi(\tau) = \begin{cases} 0, & \tau < t_0 \\ (\tau_0)^\alpha \tau^{-1-\alpha}, & \tau > t_0 \end{cases} \quad (\text{C7})$$

and

$$S(\tau) = \begin{cases} 1, & \tau < t_0 \\ (\tau_0/\tau)^\alpha \alpha^{-1}, & \tau > t_0, \end{cases} \quad (\text{C8})$$

where $t_0 = \alpha^{-1/\alpha} \tau_0$. We compute the terms I_1 , I_1^* , I_2 , and I_2^* separately. For $t \gg t_0$,

$$\begin{aligned} I_1(s) &\simeq (\tau_0)^\alpha \frac{2a}{\sqrt{\pi D}} \int_0^\infty \tau^{-1/2-\alpha} e^{-s\tau} d\tau \\ &= (\tau_0)^\alpha \frac{2a}{\sqrt{\pi D}} \frac{\Gamma(\frac{1}{2} - \alpha)}{s^{1/2-\alpha}}, \end{aligned} \quad (\text{C9})$$

which holds for $0 < \alpha < 1/2$. Alternatively, if we consider the limit $s \rightarrow 0$ in the exponential term of $I_1(s)$, $e^{-s\tau} \simeq 1$ and we have

$$I_1(s) \simeq (\tau_0)^\alpha \frac{2a}{\sqrt{\pi D}} \int_{\alpha^{-1/\alpha} \tau_0}^\infty \tau^{-1/2-\alpha} d\tau = \frac{2a\tau_0^{1/2} \alpha^{1-\frac{1}{\alpha}}}{(\alpha - 1/2)\sqrt{\pi D}}, \quad (\text{C10})$$

which holds for $1/2 < \alpha < 1$. On the other hand for $t \gg t_0$,

$$\begin{aligned} I_1^*(s) &\simeq (\tau_0)^\alpha \frac{2a}{\alpha\sqrt{\pi D}} \int_0^\infty \tau^{1/2-\alpha} e^{-s\tau} d\tau \\ &= (\tau_0)^\alpha \frac{2a}{\alpha\sqrt{\pi D}} \frac{\Gamma(\frac{3}{2}-\alpha)}{s^{3/2-\alpha}}, \end{aligned} \quad (\text{C11})$$

which holds for $0 < \alpha < 1$. With the quantities I_1 and I_1^* we can compute the mean occupation time from (C6). In particular, for $0 < \alpha < 1/2$ and using Eqs. (100), (C9), and (C11),

$$\langle \tilde{T}_1(s) \rangle \equiv \frac{I_1^*(s)}{1 - \hat{\psi}(s)} \simeq \frac{2a}{\sqrt{\pi D}} \frac{\Gamma(\frac{3}{2}-\alpha)}{\Gamma(1-\alpha)s^{3/2}}$$

and

$$\langle \tilde{T}_2(s) \rangle \equiv \frac{I_1(s)}{s(1 - \hat{\psi}(s))} \simeq \frac{2a}{\sqrt{\pi D}} \frac{\alpha\Gamma(\frac{1}{2}-\alpha)}{\Gamma(1-\alpha)s^{3/2}}.$$

Adding both terms we readily find

$$\langle T(t) \rangle \simeq \frac{2a}{\pi\sqrt{D}} \frac{\Gamma(\frac{1}{2}-\alpha)}{\Gamma(1-\alpha)} t^{1/2} \quad \text{for } 0 < \alpha < 1/2.$$

For $1/2 < \alpha < 1$ we make use of Eqs. (C10) and (C11) to get the same result for $\langle \tilde{T}_1(s) \rangle$ as above but now

$$\langle \tilde{T}_2(s) \rangle \simeq \frac{2a\tau_0^{1/2-\alpha}\alpha^{2-\frac{1}{2\alpha}}}{\sqrt{\pi D}(\alpha-1/2)\Gamma(1-\alpha)s^{1+\alpha}}$$

so that

$$\begin{aligned} \langle T(t) \rangle &\simeq \frac{2a\tau_0^{1/2}\alpha^{1-\frac{1}{2\alpha}}}{\sqrt{\pi D}(\alpha-1/2)\Gamma(1-\alpha)\Gamma(\alpha)} \\ &\times \left(\frac{t}{\tau_0}\right)^\alpha \quad \text{for } 1/2 < \alpha < 1. \end{aligned}$$

b. Mean square occupation time

We need to compute I_2 and I_2^* analogously. First, we note from Eq. (89) that

$$\langle T^2(t) \rangle_{\text{BM}} \simeq \frac{2a^2}{D} t.$$

If we consider $e^{-s\tau} \simeq 1$ in the limit $s \rightarrow 0$ the integrals in I_2 and I_2^* converge for $\alpha > 1$ and $\alpha > 2$, respectively. Then,

this approximation does not hold in our range of interest of the values of α . Instead, we consider the limit $t \gg t_0$. From Eqs. (C3) and (C7)

$$I_2(s) \simeq \frac{2a^2}{D} (\tau_0)^\alpha \int_0^\infty e^{-s\tau} \tau^{-\alpha} d\tau = \frac{2a^2(\tau_0)^\alpha}{D} \frac{\Gamma(1-\alpha)}{s^{1-\alpha}}, \quad (\text{C12})$$

which holds for $0 < \alpha < 1$. Analogously, from Eqs. (C4) and (C8)

$$I_2^*(s) \simeq \frac{2a^2(\tau_0)^\alpha}{\alpha D} \int_0^\infty e^{-s\tau} \tau^{1-\alpha} d\tau = \frac{2a^2(\tau_0)^\alpha}{\alpha D} \frac{\Gamma(2-\alpha)}{s^{2-\alpha}}, \quad (\text{C13})$$

which holds also for $0 < \alpha < 1$. The first and third terms of Eq. (C5) are of the same order and both behave as s^{-2} in the limit $s \rightarrow 0$. These terms can be added using Eqs. (C12) and (C13) to find

$$\frac{I_2^*(s)}{1 - \hat{\psi}(s)} + \frac{I_2(s)}{s[1 - \hat{\psi}(s)]} = \frac{2a^2}{Ds^2}. \quad (\text{C14})$$

Plugging Eqs. (C9), (C10), and (C11) together with Eq. (C14) into the expression (C5), we find

$$\langle T^2(t) \rangle \simeq \begin{cases} \frac{2a^2}{D} \left[1 + \frac{2\alpha\Gamma(\frac{1}{2}-\alpha)}{\pi\Gamma^2(1-\alpha)} \right] t, & 0 < \alpha < 1/2 \\ \frac{8a^2\tau_0}{\pi D} \frac{\alpha^{4-\frac{1}{\alpha}}}{(\alpha-1/2)^2\Gamma^2(1-\alpha)\Gamma(1+2\alpha)} \left(\frac{t}{\tau_0}\right)^{2\alpha}, & 1/2 < \alpha < 1 \end{cases}. \quad (\text{C15})$$

c. EB

From the definition of the ergodicity breaking parameter EB given in Eq. (82) one has

$$\text{EB} = \frac{\langle T^2(t) \rangle}{\langle T(t) \rangle^2} - 1.$$

In the long-time limit we can make use of the expressions above to find EB:

$$\text{EB} = \begin{cases} \alpha\pi - 1 + \frac{1}{2} \left[\frac{\pi\Gamma(1-\alpha)}{\Gamma(\frac{1}{2}-\alpha)} \right]^2, & 0 < \alpha < 1/2 \\ \frac{2\Gamma^2(1+\alpha)}{\Gamma(1+2\alpha)} - 1, & 1/2 < \alpha < 1 \end{cases}.$$

This is given in Eq. (83).

-
- [1] M. R. Evans, S. N. Majumdar, and G. Schehr, *J. Phys. A: Math. Theor.* **53**, 193001 (2020).
- [2] S. Gupta and A. M. Jayannavar, *Front. Phys.* **10**, 789097 (2022).
- [3] M. R. Evans and S. N. Majumdar, *Phys. Rev. Lett.* **106**, 160601 (2011).
- [4] A. Pal, A. Kundu, and M. R. Evans, *J. Phys. A: Math. Theor.* **49**, 225001 (2016).
- [5] J. Fuchs, S. Goldt, and U. Seifert, *Europhys. Lett.* **113**, 60009 (2016).
- [6] S. Eule and J. J. Metzger, *New J. Phys.* **18**, 033006 (2016).
- [7] O. Tal-Friedman, A. Pal, A. Sekhon, S. Reuveni, and Y. Roichman, *J. Phys. Chem. Lett.* **11**, 7350 (2020).
- [8] M. R. Evans and S. N. Majumdar, *J. Phys. A: Math. Theor.* **51**, 475003 (2018).
- [9] W. Wang, A. G. Cherstvy, H. Kantz, R. Metzler, and I. M. Sokolov, *Phys. Rev. E* **104**, 024105 (2021).
- [10] W. Wang, A. G. Cherstvy, R. Metzler, and I. M. Sokolov, *Phys. Rev. Res.* **4**, 013161 (2022).
- [11] V. Stojkoski, T. Sandev, L. Kocarev, and A. Pal, *J. Phys. A: Math. Theor.* **55**, 104003 (2022).
- [12] C. Godreche and J. Luck, *J. Stat. Phys.* **104**, 489 (2001).
- [13] E. B. Dynkin, *Izv. Akad. Nauk SSSR. Ser. Mat.* **19**, 247 (1955).
- [14] W. Wang, J. H. P. Schulz, W. Deng, and E. Barkai, *Phys. Rev. E* **98**, 042139 (2018).
- [15] A. Nagar and S. Gupta, *Phys. Rev. E* **93**, 060102(R) (2016).

- [16] M. Radice, *J. Phys. A: Math. Theor.* **55**, 224002 (2022).
- [17] J. Aaronson, *An Introduction to Infinite Ergodic Theory* (American Mathematical Society, Providentown, RI, 1997).
- [18] T. Akimoto and E. Barkai, *Phys. Rev. E* **87**, 032915 (2013).
- [19] E. Aghion, D. A. Kessler, and E. Barkai, *Phys. Rev. Lett.* **122**, 010601 (2019); *Chaos Solitons Fractals* **138**, 109890 (2020).
- [20] T. Akimoto, E. Barkai, and G. Radons, *Phys. Rev. E* **101**, 052112 (2020).
- [21] E. Barkai, G. Radons, and T. Akimoto, *Phys. Rev. Lett.* **127**, 140605 (2021); *J. Chem. Phys.* **156**, 044118 (2022).
- [22] S. Giordano, F. Cleri, and R. Blossey, *Phys. Rev. E* **107**, 044111 (2023).
- [23] G. Afek, N. Davidson, D. A. Kessler, and E. Barkai, *Rev. Mod. Phys.* **95**, 031003 (2023).
- [24] A. Pal, *Phys. Rev. E* **91**, 012113 (2015).
- [25] S. Ray and S. Reuveni, *J. Chem. Phys.* **152**, 234110 (2020).
- [26] B. Munsky, I. Nemenman, and G. Bel, *J. Chem. Phys.* **131**, 235103 (2009).
- [27] G. Bel, B. Munsky, and I. Nemenman, *Phys. Biol.* **7**, 016003 (2009).
- [28] J. Masoliver and M. Montero, *Phys. Rev. E* **100**, 042103 (2019).
- [29] A. S. Bodrova, A. V. Chechkin, and I. M. Sokolov, *Phys. Rev. E* **100**, 012120 (2019).
- [30] A. S. Bodrova and I. M. Sokolov, *Phys. Rev. E* **101**, 062117 (2020).
- [31] V. Méndez, A. Maso-Puigdellosas, T. Sandev, and D. Campus, *Phys. Rev. E* **103**, 022103 (2021).
- [32] S. N. Majumdar, P. Mounaix, S. Sabhapandit, and G. Schehr, *J. Phys. A: Math. Theor.* **55**, 034002 (2022).
- [33] A. A. Stanislavsky and A. Weron, *J. Phys. A: Math. Theor.* **55**, 074004 (2022).
- [34] M. Biroli, H. Larralde, S. N. Majumdar, and G. Schehr, *Phys. Rev. Lett.* **130**, 207101 (2023).
- [35] A. Vezzani, E. Barkai, and R. Burioni, *Phys. Rev. E* **100**, 012108 (2019).
- [36] A. Pal, S. Kostinski, and S. Reuveni, *J. Phys. A: Math. Theor.* **55**, 021001 (2022).
- [37] A. Altshuler, O. L. Bonomo, N. Gorohovsky, S. Marchini, E. Rosen, O. Tal-Friedman, S. Reuveni, and Y. Roichman, [arXiv:2306.12126](https://arxiv.org/abs/2306.12126).
- [38] M. Abramowitz and I. A. Stegun, *Handbook of Mathematical Functions* (Dover Publications, New York, 1972).
- [39] R. Metzler and J. Klafter, *Phys. Rep.* **339**, 1 (2000).
- [40] D. R. Cox, *Renewal Theory* (Methuen, London, 1962).
- [41] A. S. Bodrova, A. V. Chechkin, and I. M. Sokolov, *Phys. Rev. E* **100**, 012119 (2019).
- [42] J. M. Chambers, C. L. Mallows, and B. W. Stuck, *J. Am. Stat. Assoc.* **71**, 340 (1976).
- [43] A. Pal and S. Reuveni, *Phys. Rev. Lett.* **118**, 030603 (2017).
- [44] I. Eliazar and S. Reuveni, *J. Phys. A: Math. Theor.* **53**, 405004 (2020).
- [45] R. Yin and E. Barkai, *Phys. Rev. Lett.* **130**, 050802 (2023).
- [46] J. M. Meylahn, S. Sabhapandit, and H. Touchette, *Phys. Rev. E* **92**, 062148 (2015).
- [47] F. den Hollander, S. N. Majumdar, J. M. Meylahn, and H. Touchette, *J. Phys. A: Math. Theor.* **52**, 175001 (2019).
- [48] A. Pal, R. Chatterjee, S. Reuveni, and A. Kundu, *J. Phys. A: Math. Theor.* **52**, 264002 (2019).
- [49] P. C. Bressloff, *Phys. Rev. E* **102**, 042135 (2020).
- [50] P. Singh and A. Pal, *J. Phys. A: Math. Theor.* **55**, 234001 (2022).
- [51] S. Redner, *A Guide to First-Passage Processes* (Cambridge University Press, New York, 2001).
- [52] Y. He, S. Burov, R. Metzler, and E. Barkai, *Phys. Rev. Lett.* **101**, 058101 (2008).
- [53] N. R. Smith, S. N. Majumdar, and G. Schehr, *Europhys. Lett.* **142**, 51002 (2023).
- [54] N. R. Smith and S. N. Majumdar, *J. Stat. Mech.* (2022) 053212.
- [55] M. Kac, *Trans. Amer. Math. Soc.* **65**, 1 (1949).
- [56] S. N. Majumdar, *Curr. Sci.* **89**, 2076 (2005).
- [57] R. Kutner and J. Masoliver, *Eur. Phys. J. B* **90**, 50 (2017).
- [58] V. Zaburdaev, S. Denisov, and J. Klafter, *Rev. Mod. Phys.* **87**, 483 (2015).
- [59] E. Aghion, D. Kessler, and E. Barkai, *Eur. Phys. J. B* **91**, 17 (2018).
- [60] M. F. Shlesinger, *J. Stat. Phys.* **10**, 421 (1974).
- [61] S. Carmi, L. Turgeman, and E. Barkai, *J. Stat. Phys.* **141**, 1071 (2010).